An evaluation of cell transfection strategies to package RNA in small extracellular vesicles

Jenna McCann

A thesis submitted in partial fulfillment of the requirements for the
Master's of Science degree in Cellular and Molecular Medicine

Department of Cellular and Molecular Medicine
Faculty of Medicine
University of Ottawa

Abstract

Small extracellular vesicles are endogenous delivery vehicles produced by most cells. They have been shown to carry miRNA to recipient cells to modulate them. As a result, they have attracted much attention for their potential use as delivery vehicles for therapeutics. Silencing RNAs are a potent drug class but toxicity from the delivery vehicles used and the elevated doses they require prevented many clinical trials from moving forward. Additionally, their therapeutic effect is short-lived but can be extended by the addition of chemical modifications. Therefore, it is beneficial to determine a method that enables chemically stabilized siRNAs to be packaged in small extracellular vesicles. Few miRNA are packaged in these vesicles and their selective packaging is not well understood, making it difficult to promote the loading of specific siRNAs into small extracellular vesicles. Since chemically modified RNAs cannot be expressed, transfection of extracellular vesicle-producing cells was attempted to load siRNA in small extracellular vesicles. Here, we provide evidence that small extracellular vesicle preparations isolated from transfected cells contain larger particles than ones isolated from untransfected cells, suggesting that the vesicles may fuse with transfection complexes. Transfected siRNA co-localized with the late endosomes where some vesicle subtypes, called exosomes, are synthesized. This suggests that transfection complexes may accumulate in the late endosome where they may fuse with or be released alongside small extracellular vesicles. Importantly, extracellular vesicles released by transfected cells also appear to be less efficient at delivering siRNA cargoes than those produced by untransfected cells. Therefore, transfection complexes or fusions of transfection complexes and the vesicles may be a major contaminant of the preparations of small extracellular vesicles from transfected cells. This is likely a major concern as a significant amount of published literature has used transfection of cells to load RNAs in small extracellular vesicles.

Statement of contributions

My MSc thesis entitled "An evaluation of cell transfection strategies to package RNA in small extracellular vesicles" is a product of my own writing. Derrick Gibbings is responsible for the initial conceptualization of the project. I executed all protocols and analysis except for the ones listed below.

Vera Tang, the flow cytometry and virometry core facilities' manager, and Anna Fritzsche, the core facilities' support staff, performed flow cytometry of my samples to measure GFP knockdown in transfected cells. GFP knockdown of NHDF-Neo cells treated with small EVs was measured by CHEO's high throughput screening lab.

Sean Delany (William Stanford lab) supplied plasmids to Zhihao Guo (Ryan Russell lab), who created a HEK 293A GFP knock-in cell line which was used for transfection optimizations.

Ryan Reshke (Derrick Gibbings lab) performed the treatment of NHDF-Neo cells with the sEVs I provided him. Daniela Sosa (Derrick Gibbings lab) performed staining and microscopy imaging of cells I transfected with fluorescently-labeled siRNA. Derrick Gibbings prepared the microscopy image. James Taylor (Derrick Gibbings lab) created and supplied me with HEK 293T cells expressing the GFP siRNA and the NHDF-Neo cells expressing GFP.

Funding was provided by an NSERC Discovery grant awarded to Derrick Gibbings, and an Ontario Graduate Scholarship and an Alexander Graham Bell Canada Graduate Scholarship awarded to me.

The thesis presented here was read and edited by Derrick Gibbings prior to submission.

Acknowledgements

I am very grateful to Derrick Gibbings for giving me the opportunity to pursue a master's under his supervision. His guidance has been invaluable. My project took unexpected turns into uncharted territories which allowed me to develop valuable qualities such as adaptability and confidence. The challenges faced tested my perseverance and determination as well as problem solving capabilities. These qualities I've gained will be beneficial in future opportunities.

I am also thankful for my co-supervisor Carolina Ilkow and the members of my thesis advisory committee; Jocelyn Côté and Martin Pelchat, for providing me with helpful suggestions and feedback throughout my degree.

I am grateful to the neighboring labs such as the Bernard Jasmin, Ryan Russell, Jocelyn Côté, and Christine Pratt labs, that have supplied tools and reagents in times of need. The David Lohnes lab deserves particular thanks for constantly allowing me to use their electroporation system.

I am immensely grateful to the current and past members of the Derrick Gibbings lab. Past-members (Alyssa Pastic, Danielle McCulloch, Maneka Chitiprolu, Matteo Da Ros) and current members (Ryan Reshke, James Taylor, Olanta Negeri, Alexandre Savard, Maisa Alkailani, Huishan Guo, Kaela O'Connor, Daniela Sosa, Yunping Xue, Kristofferson Tandoc, Kallol Dutta) have provided helpful input and support throughout my studies. I am indebted to James Taylor, the research associate, for his guidance, knowledge and being patient in training me and answering my many questions. My lab roommates, Ryan, Alex, and James were important in creating a supportive and welcoming environment which made me feel included and accepted. Olanta also played a part in creating this encouraging and reassuring work place. The state of this work environment was crucial to my diligence and stability which played a major role in the completion of my thesis. I truly am sad to leave these friends I have made in the Derrick Gibbings lab however, hope to keep in touch with them.

Lastly, I am thankful for my friends and family who have supported me through graduate school and helped me balance work and life. My parents have been a significant part of my support system and played an integral role in my success and achieving the goals I have.

Table of contents

List of tables

List of figures

List of abbreviations

2’-O-me	2’-O-methyl
2’F	2’ fluorine
A_{260}	Absorbance at 260 nm
Ago	Argonaute
Arc	Activity-regulated cytoskeleton-associated protein
C_q	Quantitation cycles
ds	Double strand or double stranded
EV(s)	Extracellular vesicle(s)
Geo-MFI	Geometric mean fluorescence intensity
GFP	Green fluorescent protein
HnRNP	Heterogeneous nuclear ribonucleoprotein Q also known as SYNCRIP
HuR	ELAV-like protein 1
LNP(s)	Lipid nanoparticle(s)
Min	Minute(s)
MIQE	Minimum information for publication of quantitative real-time PCR experiments
miRNA(s)	MicroRNA(s)
mRNA(s)	Messenger RNA(s)
nt	Nucleotide(s)
NTA	Nanoparticle tracking analysis
PDL	Poly-D-lysine
Pol II	RNA polymerase II
qPCR	Quantitative polymerase chain reaction
RISC	RNA-induced silencing complex
RNAi	RNA interference
Rpm	Revolutions per minute
RT	Reverse transcription or room temperature
sEV(s)	Small extracellular vesicle(s)

siRNA(s)	Silencing or short interfering RNA(s)
SOD1	Superoxide dismutase
ss	Single strand or single stranded
TC	Transfection complexes
TTR	Transthyretin
WT	Wild-type

Introduction

Silencing RNA

Mechanism of siRNA

Silencing RNA (siRNA) are short double stranded RNAs that mimic endogenous microRNA (miRNA). miRNA and siRNA regulate gene expression by binding complementary mRNA sequences to inhibit translation. This biological process is termed RNA interference (RNAi). The canonical biosynthesis of miRNA involves pri-miRNA transcripts getting cleaved by Drosha to release a pre-miRNA hairpin which is exported out of the nucleus (**Figure 1a**). Once in the cytoplasm, it is processed by Dicer to form a ~21 nucleotide double stranded (ds) RNA, with 3' overhangs and 5' monophosphates[1], which is then loaded into Argonaute (Ago), an essential component of the RNA-induced silencing complex (RISC). Once the miRNA is loaded into Ago, one of the strands of the miRNA-passenger strand duplex is selectively removed. The now mature single stranded miRNA will guide Ago to a complementary mRNA sequence leading to mRNA degradation and repressed translation. When siRNAs are introduced into cells, they follow the miRNA pathway by binding Ago, much like the resulting dsRNA produced after processing by Dicer. siRNA can be synthesized to be perfectly complementary to target mRNA, which allows Ago2 to enzymatically cleave target mRNA, resulting in high potency and specificity. This has resulted in the use of siRNA as a research tool and therapeutic.

Chemical modifications of siRNA

miRNA and siRNA can be recycled to repeatedly target new mRNAs. However, their effect diminishes over 1 to 4 weeks in non-dividing cells due to degradation and even less in rapidly dividing ones due to dilution caused by cell division[2–4]. The addition of chemical

.

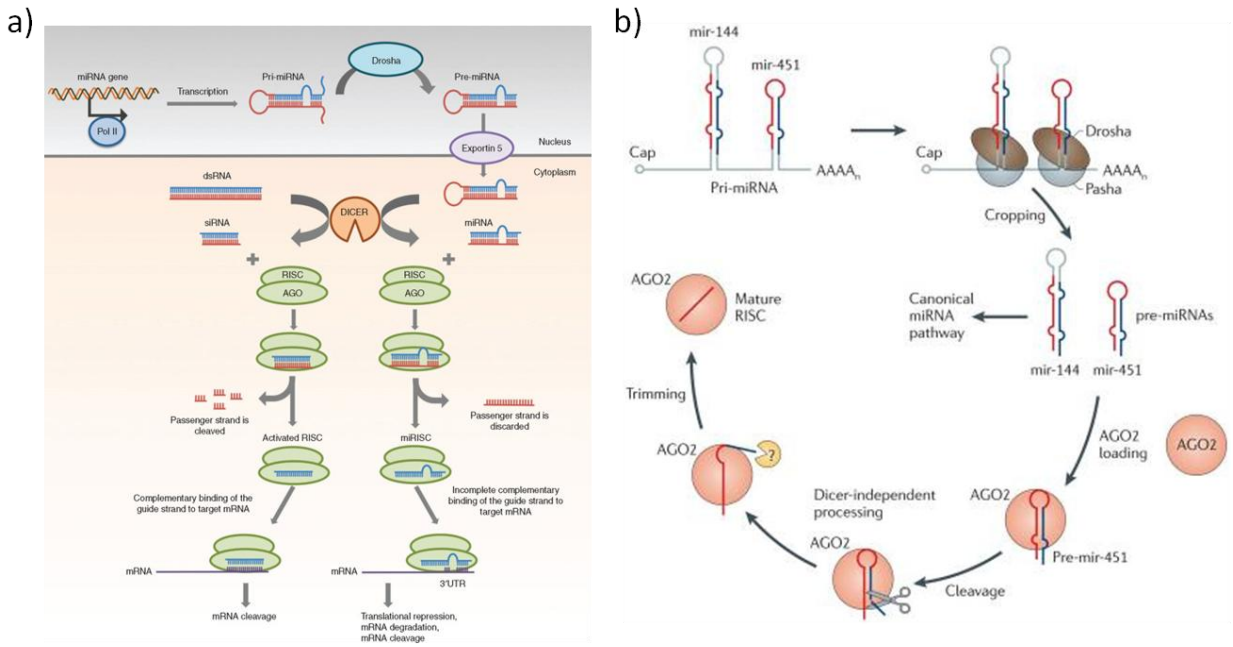

FIGURE 1. Maturation and silencing mechanism of siRNA and miRNA (a) Canonical pathway (Reprinted by permission from The American Society of Gene and Cell Therapy)[5]. (b) Dicer-independent pathway undertaken by miR-451. (Reprinted by permission from Springer Nature : Macmilan Publishers Nature Reviews Genetics Small RNA sorting: matchmaking for Argonautes, Benjamin Czech and Gregory J. Hannon, 4696110075521 (2011))[1]. Pol II, RNA polymerase II; AGO; Argonaute; RISC, RNA-induced silencing complex.

modifications to siRNAs can be used to increase stability and specificity[6–8]. These in turn extend silencing effects, and even more so in cells with slow rates of turnover

Alnylam Pharmaceuticals have shown that siRNA containing a combination of phosphorothioate linkages, and 2'-O-methyl (2'-O-me) and 2' fluorine (2'F) ribonucleoside modifications can increase the duration of target knockdown to many months in patients (**Figure 2**)[9]. 2'-O-methylations are naturally occurring post-transcriptional RNA modifications[1,10]. They have been mapped to ribosomal RNA, small nuclear RNA, transfer RNA and messenger RNA in humans. Additionally, 2'-O-me modifications protect the 3' end of Piwi-interacting RNA from degradation by preventing uridylation, which marks small RNAs for degradation[1].

Delivery of siRNA

There are many disadvantages to using naked siRNA as therapeutics in patients. Firstly, siRNA are vulnerable to serum nucleases[11,12]. Secondly, the negative charge of the backbone causes poor cell internalization since the siRNAs struggle to interact with the cell membrane which is also negatively charged. The charge also hinders interaction of the siRNAs with serum proteins, leading to its rapid clearance from blood[13]. Lastly, siRNAs can stimulate an immune response[8,14].

Studies have demonstrated that ~300 siRNA copies are required to knockdown an mRNA target by 50%[15,16] and ~2,000 siRNA copies for 80% silencing[15,17]. Therefore to achieve these high numbers of cytoplasmic siRNA and bypass the challenges listed above, siRNAs need to be packaged into delivery vehicles.

ONPATTRO (Patisiran) is the only existing FDA-approved RNAi therapy and was only approved just last year. It consists of an siRNA targeting transthyretin (TTR) delivered by lipid

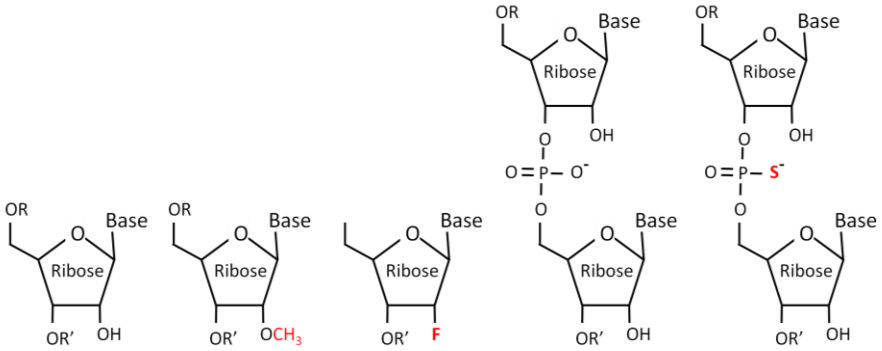

FIGURE 2. RNA modifications of ribose and nucleoside bonds. 2'-O-methyl and 2'-fluoro are RNA modifications of the sugar. Phosphorothioates are modifications of the bonds which link the nucleosides.

nanoparticles (LNP) for treatment of hereditary amyloidosis. LNPs are synthetic and associated with dose-limiting toxicity and immunogenicity[18]. This is demonstrated clearly by ONPATTRO's need for a pre-treatment with corticosteroids, acetaminophen and histamine blockers to minimize adverse events. LNP have been shown to deliver less than 1% of siRNA into the cytoplasm of cells[15,17,19,20]. Therefore, this signifies that high doses of siRNA and their delivery vehicles are required to treat patients which can lead to toxicity and has halted multiple clinical trials of siRNA[21,22]. Additionally, siRNA and LNPs largely accumulate in the liver[23,24] which restricts their use to treating diseases caused by proteins expressed in the liver. For example, in the case of ONPATTRO, the target (TTR) is mostly synthesized in the liver.

Naturally occurring endogenous lipid nanoparticles, called extracellular vesicles, seem to be able to achieve delivery of RNA to organs other than the liver[20,25] and deliver 10X times better than commercially available lipid nanoparticles[20]. Therefore, extracellular vesicles may enable safer and more efficient delivery of siRNAs if siRNAs can be packaged inside them.

Extracellular vesicles

Extracellular vesicle biogenesis

Extracellular vesicles (EVs) are particles defined by a lipid-bilayer that are non-viral, or cannot replicate and are naturally released from cells. Most cells can produce three general types of extracellular vesicles: exosomes, microvesicles, and apoptotic bodies (**Figure 3a**)[26]. The biogenesis, size, markers and content of these vesicles vary. Apoptotic bodies are 500-2,000 nm in size and contain cell organelles and nuclear fractions. These large EVs are typically released by dying cells. Microvesicles are smaller than the latter. They range between 50 and 1,000 nm and are formed by the outward budding of the plasma membrane. Exosomes, however, are generated by the inward budding of the late endosome to form multivesicular bodies (MVB).

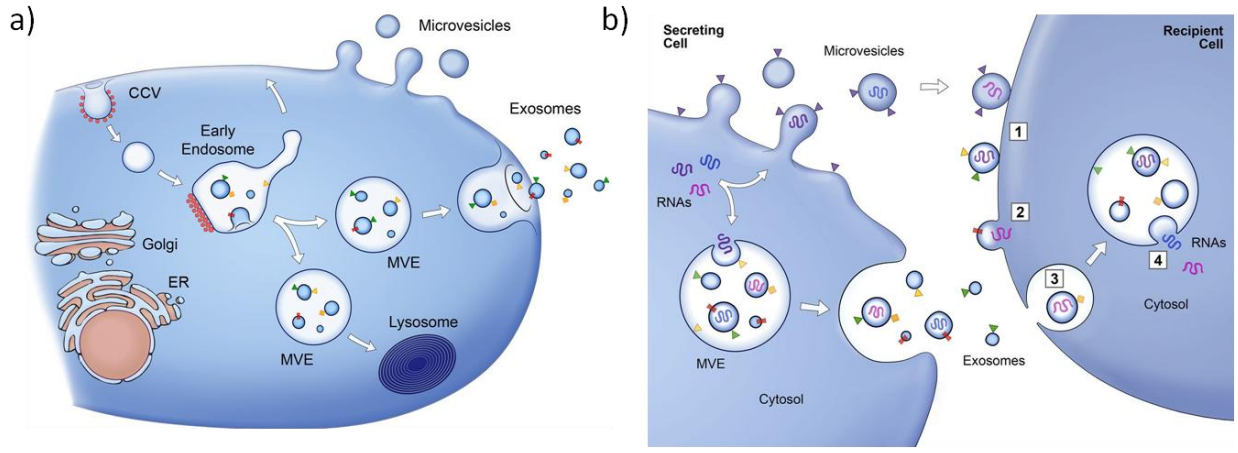

FIGURE 3. Extracellular vesicle biogenesis and cargo delivery. (a) Biosynthesis (Republished with permission of Rockefeller University Press, from Extracellular vesicles: Exosomes, microvesicles, and friends, Raposo G & Stoorvogel W, 200, 4, 2013; permission conveyed through Copyright Clearance Center, Inc.)[27]. Microvesicles release from the outward budding of the plasma membrane. Inward budding of the endosome creates multivesicular endosomes/bodies which, when fused with the plasma membrane, release vesicles called exosomes. Transmembrane proteins can be found on the surface of both types of extracellular vesicles (triangles and rectangles). CCV, clathrin-coated vesicles; ER, endoplasmic reticulum; MVE, multivesicular endosome. (b) Delivery (Republished with permission of Rockefeller University Press, from Extracellular vesicles: Exosomes, microvesicles, and friends, Raposo G & Stoorvogel W, 200, 4, 2013; permission conveyed through Copyright Clearance Center, Inc.)[27]. Extracellular vesicles such as exosomes and microvesicles interact with the cell membrane to initiate a cellular response. They may deliver their content by fusing directly with the membrane or through endocytosis. Endocytosed extracellular vesicles must fuse with the endocytic compartment to deliver their RNA and proteins into the cytosol of recipient cells.

The MVB then fuses with the plasma membrane to release the vesicles, exosomes, into the extracellular space. Exosomes are generally smaller (40-120 nm) than microvesicles although, there is an overlap in their sizes. More recently additional types of EVs have been described including exomeres, migrasomes, and Arc-containing EVs. Exomeres are approximately 35 nm in size and their biogenesis mechanism is unknown[28]. Migrasomes are formed at the tips or intersection of refraction fibers which are synthesized by migrating cells[29]. These vesicles have diameters up to 3 µm and are released upon breaking of refraction fibers. Other vesicles have been shown to traffic neural Arc mRNA which is required for synaptic plasticity. These EVs contain Arc protein which forms viral-like structures around the Arc mRNA[30,31]. Together, this demonstrates the heterogeneity of EVs.

Extracellular vesicle delivery

EVs contain RNAs and proteins encapsulated by their lipid bilayer[26]. Molecules on the surface of EVs may interact with target cell receptors to modulate a response (**Figure 3b**). The EVs may also fuse with the plasma membrane to release their content into the target cell's cytoplasm or they may be endocytosed where their membrane may fuse with the endosomal membrane to again release their cargo into the cytoplasm. Alternatively, the endocytosed EVs may be trafficked to lysosomes for degradation. These interactions enable EVs to produce a functional biological effect on the recipient cells.

Many studies have demonstrated the role of EVs in intercellular communication particularly in their ability to regulate gene expression through delivery of endogenous miRNAs[32]. Therefore, EVs could be engineered to deliver specific siRNA to treat diseases. Also, EVs are abundant in bodily fluids[27,33]. Thus, routinely administered medical procedures

involving the transfer of body fluids to others, such as blood transfusions, suggest that EVs may be safe as therapeutics or therapeutic delivery vehicles.

Extracellular vesicle isolation and characterization

Many methods exist for isolating EVs such as immunocapture, tangential flow filtration, differential centrifugation and density gradients[34]. Many available commercial kits isolate EVs through immunocapture, targeting proteins that have been shown to be associated with them. For example CD9, CD81 and CD63 are tetraspanins reported on smaller EVs[34]. However, according to the International Society for Extracellular Vesicles (ISEV), there are no markers that can distinguish subsets of EVs from each other because EVs are heterogeneous[34]. Proteins unique to EV subtypes may be specific to species, cells or experimental conditions. Therefore, isolation by targeting specific EV markers is unlikely to capture all EVs within that subtype thus, despite their high yield, using these kits results in isolation of select EV population(s) which are often contaminated with other material[35,36]. Tangential flow filtration separates molecules/particles according to their molecular size. This technique is less labor-intensive than differential centrifugation and allows filtration of large volumes. Differential centrifugation involves using different speeds to sediment various particles according to their mass. Despite, its low recovery, it is the method most used to isolate EVs[34]. It is important to note that isolated material generally contains a mixture of EVs in which the composition varies depending on the separation protocol used[34]. Additionally, the extracellular milieu is complex and contains protein complexes and lipoproteins similar in size to EVs that may result in their co-purification using many methods[34]. Therefore, the use of several proteins expected and not expected to be present in EVs should be tested to characterize EVs. Other methods are suggested in combination with western blot for EV proteins to establish which EVs are being studied. These methods include nanoparticle tracking

analysis, electron microscopy (EM), and content profiling to categorize EVs by their size or components.

As it is difficult to isolate EVs from a particular biogenesis pathway, unless visualized at the precise moment of release or by inhibiting a EV biogenesis pathway and showing that functional effects disappear, the ISEV urges authors to define EVs by their physical characteristics and isolation procedures rather than a presumed pathway of biogenesis[34]. Therefore, this thesis will use physical characteristics to define EVs as suggested by the ISEV. Going forward, particles < 200 nm detected after differential centrifugation will be termed small EVs.

Loading siRNA in small extracellular vesicles

Some RNA species found in abundance in small EVs (sEVs) are at low levels in sEV-producing cells suggesting the involvement of a highly selective packaging mode[32,37]. This mechanism and selection process is not well understood thus, making it difficult to promote the loading of specific siRNAs into sEVs. Additionally, few miRNAs are packaged in sEVs normally; on average 1 copy of a specific miRNA per 100 sEVs[38]. As between 300-2,000 copies of siRNA are required per cell to silence a target mRNA, sEVs must be highly efficient at naturally delivering their cargoes. Also, only the most abundant miRNA in sEVs are likely to be present in sufficient numbers in sEVs to have a physiological function. Therefore, for sEV delivery of siRNA to have a therapeutic effect, siRNA will need to be packaged into sEVs at levels at least similar to the most abundant miRNA in sEVs. Various methods have been attempted to load RNA into sEVs such as directly transfecting sEVs with siRNA[39,40], or transfecting[41–45] or over-expressing[20] siRNA in sEV-producing cells. RNAs transfected or

expressed in cells can be modified to contain certain sequence motifs[46–48] or structures[20] to promote their sequestration into sEVs.

Transfection of small EVs

Electroporation of small EVs (sEVs) has been previously attempted[39,40]. However, it was later shown that electroporation of sEVs did not lead to the introduction of RNA in the sEVs but instead caused their aggregation outside of the sEVs [20,49]. This resulted in co-precipitation of RNA with the sEVs during ultracentrifugation. Reshke et al. also demonstrated that miRNA endogenous to sEVs (miR-106a and let-7a) become sensitive to nucleases once electroporated, indicating that electroporation compromises the membranes of sEVs. This is supported by the fact that smaller particles, suspected to be sEV fragments, were detected by nanoparticle tracking analysis after electroporation of sEVs. This is expected as cell mortality is one of the known disadvantages of electroporation. Disruption of sEV membranes can hinder the ability to deliver. This was demonstrated by lack of knockdown of an siRNA target when EVs were electroporated compared to unelectroporated ones.

Commercially available kits claim to transfect sEVs. Although their mechanisms are not disclosed, we can assume that the components affect the sEVs to package something in them. If these components consist of cationic lipids such the common transfection reagents, fusion of liposomes and sEVs can cause the formation of large hybrid vesicles and likely alters the sEVs and their ability to deliver[50]. This could lead to making false assumptions about sEV delivery.

Stable or transient over-expression of siRNA in small EV-producing cells

Over-expression of RNA sequence motifs

Some RNA motifs were shown to be enriched in small EVs (sEVs). Villarroya-Beltri et al. identified two motifs (GGAG and CCCU) that were over-represented in sEV miRNA[46]. Mass spectrometry of proteins pulled-down by sEV miRNA-coated beads identified several

heterogeneous nuclear ribonucleoproteins (hnRNPs); including hnRNPA2B1 and hnRNPA1. Mutations of these motifs or changes in expression of these hnRNPs affected levels of specific miRNAs in sEVs. Additionally, hnRNPA2B1 co-localized with multivescular bodies (MVB) and was also found in sEVs with hnRNPA1. Similarly, proteins were isolated from hepatocyte lysate mixed with beads coated with miRNAs enriched in hepatocyte sEVs[47]. Mass spectrometry revealed hnRNP-Q (also known as SYNCRIP). The GGCU motif was found in miRNAs bound by hnRNP-Q. In stressed Huh7 cells, HuR uncouples miR-21 and miR-122 from Ago2 and binds them to shuttle them away from P-bodies for extracellular export to control the stress response[48]. HuR binds AU rich sequences but is also thought to bind GU rich sequences which are found in these miRNAs. HuR was also found in MVB fractions. Therefore, RNAs including sequence motifs could be designed to promote their packaging in sEVs. Nonetheless, including a sequence motif in short siRNA may lead to reduced specificity and potency of the siRNA towards its target.

Over-expression of RNA structures

MiR-451 has been shown to be 500-10,000 fold enriched in small EVs (sEVs) compared to their originating cells, suggesting that it is selectively packaged into sEVs[20,37]. This miRNA does not follow the canonical miRNA maturation process described above[20,51–53]. The 42 nt Drosha-processed pre-miR-451 stem-loop is too short to bind Dicer in the cytoplasm and thus bypasses cleavage by Dicer (**Figure 1b**). The hairpin is instead directly loaded into Ago2 where the distal strand is cleaved to generate a ~30 nt product. Exonucleases digest the tail of this product to form the ~22 nt mature miR-451. Various studies proposed that expression of a pre-miR-451, with its uniquely short hairpin structure preserved but sequence altered to include other miRNA or siRNA sequences, would be processed through this same Dicer-independent pathway

to form a mature miRNA/siRNA[52,53]. Hypothetically, this could result in the miRNA/siRNA sequence inserted in the pre-miR-451 hairpin being selectively packed into sEVs like miR-451.

Reshke et al. produced stable cell lines over-expressing the pre-miR-451 RNA structure containing new siRNA sequences, such as a SOD1-targeting siRNA, to exploit this selective sEV packaging mechanism[20]. They demonstrated that siRNAs could be enriched 78 to >7,000 fold in sEVs compared to the sEV producing cells, which did not occur when the siRNA was expressed from another pre-miRNA backbone (pre-miR-16). Copy numbers of these siRNAs in sEVs reached up to 1 copy per small EV which is similar to the most abundant miRNAs in sEVs. The sEVs were able to reduce expression of target genes in primary cells in culture and in mice with 10-fold less siRNA than lipid nanoparticles, showcasing the efficient delivery capacity of sEVs. However, RNA packaged in sEVs through the expression of pre-miR-451 are not chemically modified since RNA containing synthetic chemical modifications cannot be stably or transiently expressed. This would lead to a target knockdown of only days or weeks rather than months if this was ever to be used as a drug in patients. Therefore, chemically modified siRNA in a pre-miR-451 backbone may only be introduced into sEVs through transfection of sEV-producing cells.

Transfection of small EV-producing cells with siRNA

Transfection of small EV-producing cells has been frequently performed to package RNA into small EVs (sEVs)[41,43]. Transfection can be achieved using many methods; chemical, physical and virus-based. Virus-based methods are typically used for stable or transient expression thus, are not a viable option for loading chemically enhanced siRNA into sEVs.

Chemical transfection

The two most common reagent-based methods for transfecting cells are lipid-based or polymer-based reagents. Cationic lipids are amphiphiles that form liposomes, leaving the positively charged head exposed on the outside (**Figure 4**)[54]. The positive charge interacts with the negatively charged phosphate backbone of nucleic acids to form transfection complexes. The positive charge of the lipids also facilitates interactions with cell membranes which are also negatively charged. Transfection complexes internalized through endocytosis must escape the endosome for siRNA to reach the cytoplasm and induce an effect, or in our interest, be released by sEVs. An example of this type of reagent is Lipofectamine RNAiMAX. Other reagents, such as RiboJuice and INTERFERin siRNA are non-liposomal. RiboJuice is made of a mixture of cationic polyamines (a class of polymers) and lipids. Polymers can be synthesized into various structures; linear, branched, or spherical. The positive charge of polymers interacts with nucleic acids and cell membranes as described for the lipids. According to the manufacturer's customer service, INTERFERin uses non-liposomal cationic amphiphiles, suggesting that polymers are used instead of lipids.

Physical transfection

Physical transfection forces entry of nucleic acids by high velocity (biolistic), magnetic field (magnetofection), piercing the membrane with an injector (microinjection), or permeabilizing the cell membrane with an electric field (electroporation) or laser (laser/optifection). These methods require specific instruments and most are not scalable to transfecting the millions of cells necessary for sufficient sEV production for use as therapeutics.

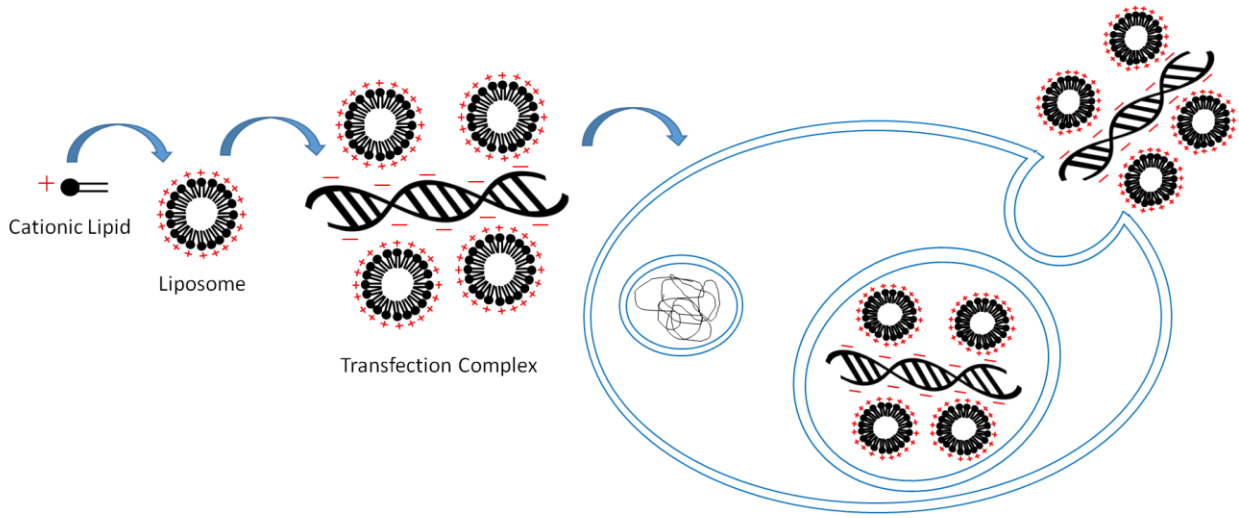

FIGURE 4. Lipid-based transfection mechanism. Cationic lipids are amphiphiles which posses a positively charged head group linked to an apolar hydrophobic body typically consisting of the 2 carbon chains. The lipids associate to form a liposome. The nucleic acids are not encapsulated within these rather; the positive charge of the liposome interacts with the negatively charged nucleic acids and condenses them thus, forming transfection complexes. These transfection complexes are thought to enter the cell through endocytosis. They must escape the endosomal pathway in order to regulate gene expression.

Thesis objective and overview

This thesis aims to determine whether chemically modified RNAs can be packaged into small extracellular vesicles (sEVs) (< 200nm) by transfecting sEV-producing cells. These RNAs include a pre-miR-451 RNA hairpin containing the sequence for a mature siRNA, a mature single stranded siRNA, and a strand complementary to the mature siRNA which will be annealed to the mature strand to form a double stranded siRNA. The RNAs contain 2'-O-methyl, 2'fluorine and phosphorothioate modifications and will be transfected and compared to their unmodified counterpart.

As a therapeutic target in this project, the human superoxide dismutase 1 (*SOD1*) mRNA was selected. Over 170 evenly distributed mutations have been identified in the SOD1 gene and these are among the most common genetic causes of Amyotrophic Lateral Sclerosis (ALS)[55]. ALS is a disease characterized by the rapid and progressive loss of motor neurons which leads to muscle weakness then paralysis, typically resulting in death 3-5 years after diagnosis. ALS is incurable and the two treatments available do not substantially increase survival and only benefit a subset of people with ALS[56,57]. Mutated SOD1 is thought to misfold and cause the formation of inclusions, with native and mutated SOD1 proteins, which themselves spread in a prion-like fashion to cause pathogenesis[55]. Preventing accumulation of SOD1 through siRNAs has been shown to slow disease progression in ALS mouse models[58,59]. Delivery of chemically modified RNAs targeting SOD1 through sEVs could help treat diseases like ALS, by enabling safe, long-term silencing of mRNAs like SOD1.

Packaging these small RNAs into sEVs by transfecting sEV-producing cells was tested. The characteristics of sEV preparations produced from transfected cells suggest that sEVs fuse with transfection complexes, or transfection complexes may accumulate in late endosomes and then be released alongside sEVs from cells. Therefore, transfection complexes or fusions of

transfection complexes and sEVs may be a major contaminant of sEV preparations from transfected cells. This is likely a major confounding factor in a significant amount of published literature and suggests that it is very challenging to monitor small RNA delivery by sEVs by transfecting the sEV-producing cells.

Materials and Methods

Cell lines

(1) NSC-34 (Cedarlane)

(2) HEK 293T (ATCC)

(3) HEK 239A expressing GFP. This cell line was synthesized by Zhihao Guo of the Dr. Ryan Russell lab (University of Ottawa). emGPF was knocked-in with CRISPR technology. The sequence for a guide RNA targeting the AAVS1 locus (AAVS1 gs2, 5'GTCACCAATCCTGTCCCTAG3') was cloned into pSpCas9(BB)-2A-Puro (PX459) V2.0 (Addgene, 62988) by Dr. Sean Delaney from the Dr. William Stanford lab (University of Ottawa/Ottawa Hospital Research Institute). The donor plasmid, also synthesized by Dr. Sean Delaney, consists of an emGFP-T2A(self-cleaving peptide)-Zeocin transgene, flanked by regions of homology to AAVS1, cloned into a pUC19 (Addgene, 50005).

(4) HEK 293T expressing GFP siRNA. The creation of this stable cell line was synthesized as described by Reshke et al.. In short, a G-block (IDT, 5'AGATCTTACTGACTGCCAGGGCACTTGGGAATGGCAAGGATGAACTTCAGGGTCAGCTTGCGTTGACCCTGAAGTTCATTCTTGCTATACCCAGAAAACGTGCCTTTTTGGTACCAAGCTT3') was cloned into pSilencer 2.1-U6 (Puromycin) (Invitrogen, AM5762M) to encode a pre-miR-451 reprogrammed to express GFP siRNA (5'ATGAACTTCAGGGTCAGCTTGC3'). The coding region of the reprogrammed pre-miR-451 from pSilencer 2.1-U6, a fragment of pGIPZ (Dharmacon) encoding all components of a lentiviral transfer vector, a fragment of pXPAC-luc (Systems Biosciences) encoding luciferase, and a fragment of pGIPZ encoding an IRES site and the puromycin resistance gene were amplified by PCR and combined into a single vector by Gibson assembly. The resulting vector was transfected with pMD2.G (Addgene,12259) and psPAX2

(Addgene,11260) into HEK 293T where expression of luciferase, puromycin resistance and the reprogrammed pre-miR-451 construct occurred from a CAG enhanced CMV promoter. Lentiviral particles produced from the transfected HEK 293T were ultracentrifuged, diluted and added to HEK 293T cells in culture, thus producing HEK 293T expressing GFP siRNA, which were selected with puromycin 3 days post-transduction.

(5) NHDF-Neo expressing GFP. The pLVX-AcGFP1-N1 vector (Clontech, 632154) encoding AcGFP1 was transfected into HEK 293T with pMD2.G and psPAX2. Lentiviral particles produced from the transfected cells were ultracentrifuged, diluted and added to neonatal normal human dermal fibroblasts (NHDF-Neo) (Cedarlane, CC-2509) in culture thus, producing NHDF-Neo expressing GFP, which were selected with puromycin 3 days post-transduction. GFP fluorescence was confirmed in all cells with ZOE fluorescent cell imager (Bio-Rad, 1450031).

Cell culture

Cells were cultured in DMEM (Wisent Bioproducts, 319-015-CL) supplemented with 10% heat inactivated FBS (Wisent Bioproducts, 081-150) and 1% Penicillin-Streptomycin (Wisent Bioproducts, 450-201-EL). Cells were cultured at 37°C 5% CO_2 in humidified incubators. Cells were dissociated/passaged using Trypsin/EDTA (0.25%/EDTA 2.21 mM in HBSS) (Wisent Bioproducts, 325-043-EL) proceeding a 1X PBS wash (pH 7.4, without calcium and magnesium) (Wisent, 311-010-CL). The trypsin was neutralized with at least equal volume of culture media. The concentration of cell suspensions was determined using a hemacytometer (Sigma, Z359629 or Thermo Fisher Scientific, 0267110).

siRNAs

Chemically modified SOD1-targeting RNAs contained a specific pattern of enhancements which include 2'fluorine, 2'-O-methyl and phosphorothioate modifications.

TABLE 1: Transfected small RNA sequences

Name	Sequences (5'→ 3')
SOD1 siRNA in pre-miR-451 backbone	PUUCAGUCAGUCCUUUAAUGCUUAUUAAAGGACUGACUGAUUC
SOD1-targeting ssRNA	PUUCAGUCAGUCCUUUAAUGCUU
SOD1 siRNA	ssSOD1 siRNA is annealed to a complementary strand (5'AGCAUUAAAGGACUGACUGAA 3') at a 10μM concentration in 10X T4 DNA Ligase Reaction Buffer (NEB, B0202S) with a final reaction volume of 100μL during a 10min incubation at 95°C, with a gradual cool down of 0.1°C/sec to 25°C for 1min.
GFP siRNA	5'AUGAACUUCAGGGUCAGCUUGC 3' (IDT) 5'AAGCUGACCCUGAAGUUCAUU 3' (IDT) Annealed as described above.
Scramble siRNA	Silencer Select Negative Control No.2 siRNA (Thermo Fisher Scientific, 4390846)
siGLO Cyclophilin B siRNA	siGLO Cyclophilin B Control siRNA fluorescently labeled with DY-547 (Human/Mouse/Rat) (Dharmacon, D-001610-01-05)

P = 5'phosphate

Transfection

Transfection of SOD1-targeting RNA

NSC-34 cells were grown to 60-80% confluence in 10cm dishes and transfected with Lipofectamine RNAiMAX (Thermo Fisher Scientific, 13778150) and Opti-MEM (Thermo Fisher Scientific, 31985-070) as seen below for a final concentration of 10 nM of SOD1 siRNA in 6 mL of antibiotic-free DMEM supplemented with 1% heat inactivated FBS.

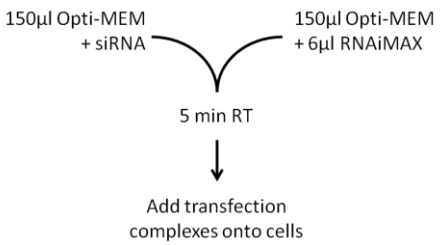

Transfection of GFP siRNA was tested in parallel. Twenty four hours post-transfection culture media was removed and cells were washed with 1X PBS to remove any remnants of contaminating small EVs originating from the FBS in the DMEM. UltraCULTURE Serum-free Media (Lonza, BE12-725F) supplemented with 1% Penicillin-Streptomycin and 1% L-glutamine (Thermo Fisher Scientific, 25030-081) was added to the cells. The following day the UltraCULTURE from 2 plates transfected with the same SOD1-targeting RNA was collected and combined for isolation of small EVs by differential centrifugation. Cells were combined with 1 mL Trizol Reagent for RNA isolation for RT-qPCR and northern blots.

Optimizing transfection with GFP siRNA

Five hundred thousand HEK 239A GFP cells were seeded per well of a 6-well plate. Similar amounts of HEK 293T were seeded as a control. HEK 293A GFP cells were transfected with GFP siRNA using 4 methods: electroporation and 3 different chemical reagents; Lipofectamine RNAiMAX, INTERFERin (VWR, 89129-930) and RiboJuice (Millipore Sigma, 71115-4). Untransfected HEK 239A GFP acted as a control. The manufacturers' recommended protocol for transfection of a well of a 6-well plate was followed (see below).

RNAiMAX

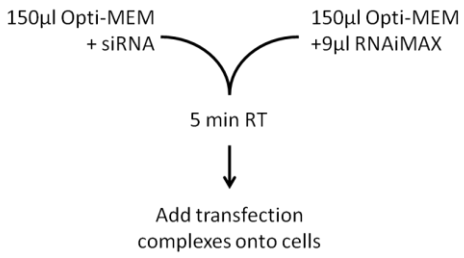

INTERFERin

RiboJuice

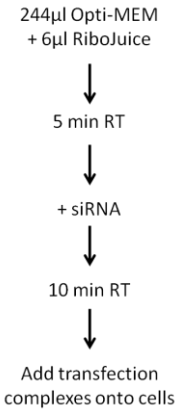

Electroporation

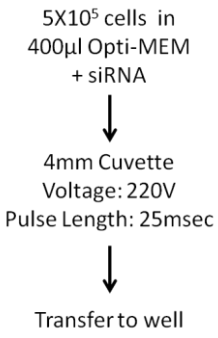

Various concentrations of GFP siRNA and scramble siRNA were transfected: 1 nM, 5 nM and 10 nM in a final volume of 2 mL DMEM supplemented with 10% heat inactivated FBS and 1% Penicillin-Streptomycin. The GFP and scramble siRNA were added alone at a final concentration of 10 nM without any transfection reagent to control for the effects caused by the reagents. Additionally, cells were electroporated without siRNA to control for the effects caused by electroporation. Cells required pelleting at 400 xg for 5min then resuspension in Opti-MEM prior to electroporation with Gene Pulser Xcell Electroporation Systems (Bio-Rad, 1652661). The pre-programmed protocol for transfection of HEK 293 in a 2 mm cuvette was followed. However, voltage was doubled as the cuvette size used was 4 mm (Bio-Rad, 1652081). Electroporated samples were hastily transferred to pre-warmed plated-media. Electroporation cuvettes were washed between uses with sterile nuclease-free water, soaked in 75% EtOH and again rinsed with sterile nuclease-free water. An experiment using new cuvettes to electroporate 5 nM of GFP siRNA in HEK 293A GFP was done additionally to compare knockdown of the reused cuvette with new ones. Twenty-four hours post-transfection, the culture media was replaced with fresh. Two days and three days post-transfection, cells were collected for flow cytometry.

GFP knockdown when media is changed 6 hours or 24 hours post-transfection

HEK 239A GFP were seeded and transfected as described above with RNAiMAX and a final concentration of 10 nM of GFP siRNA. Untransfected HEK 239A GFP and HEK 293T acted as controls. Media was changed 6 hours or 24 hours post-transfection. Three days post-transfection, cells were collected for flow cytometry.

Packaging GFP siRNA via optimized transfection conditions

Transfection was scaled to 15cm plates (15mL) for sufficient production of small EVs; 7.5 time the volume of a well of a 6-well plate. Thus, 7.5 times more cells were seeded ($3.75x10^6$) and 7.5 times more Opti-MEM and transfection reagent was used; RNAiMAX (1,125 µL X2 Opti-MEM + 15 µL 10µM siRNA + 67.5 µL RNAiMAX), INTERFERin (1.5 mL Opti-MEM + 15 µL 10 µM siRNA + 60 µL INTERFERin), and RiboJuice (1,830 µL Opti-MEM + 15 µL 10 µM siRNA + 45 µL RiboJuice). For electroporation, seeded cells were lifted, centrifuged and resuspended in 400 µL of Opti-MEM. Fifteen microliters of 10 µM siRNA was introduced to a cuvette containing the cell suspension. Electroporation was followed as described above. The DMEM was changed to UltraCULTURE 6 hours post-transfection after a 1X PBS wash. The UltraCULTURE was collected three consecutive days following transfection. Therefore, the day following transfection with the various methods, the UltraCULTURE was collected and replaced with fresh UltraCULTURE. The collected media underwent the first two centrifugations of the differential centrifugation protocol then, was stored at 4°C. The next day, the UltraCULTURE was again collected and replaced, centrifuged but then pooled with the previous day's centrifuged collection and stored at 4°C. The 3rd day after transfection, UltraCULTURE was collected, centrifuged and pooled with the previous days' centrifuged collections. The differential centrifugation protocol then was continued to isolate small EVs.

Co-localization of siRNA and CD63

Fifty thousand HEK 293T cells were seeded on PDL-coated cover slips (Millipore Sigma, P7280-5MG). The cells were transfected with siGLO (Dharmacon, D-001610-01-05) at a 10 nM concentration in 1 mL of media and RNAiMAX at the levels recommended for a well of a 12 well plate. Media was changed 24 hours after transfection accordingly. Cells were fixed 72, 48, 24 and 6h after transfection with 4% PFA in PBS for 10min at room temperature. Cover slips were washed with 1X PBS thrice then stored at 4°C until CD63 staining.

Comparing sEVs from transfected and untransfected cells

Fifteen centimeter plates of HEK 293T were left untransfected or transfected with GFP siRNA and RNAiMAX with the method above. Media change and ultaCULTURE collections also followed statements listed above. When a spike-in is indicated, the centrifuged media collected from three consecutive days is split in 2 where PBS is added or half of the amount of transfection complexes initially transfected is added.

GFP siRNA delivery by sEVs originating from transfected and untransfected cells

$7.5x10^6$ HEK 293T expressing GFP siRNA in 15cm dishes were left untransfected or transfected with RNAiMAX and a scramble siRNA with the method described above. Untransfected HEK 293T acted as a control. Media change and ultaCULTURE collections also followed statements listed above.

Flow cytometry

Cells were detached with trypsin and neutralized with culture media. The suspension was centrifuged at 300 xg for 5 min and the cell pellet was resuspended in 1% FBS in 1X PBS. The cell suspension was diluted to a concentration of 10^6 cells/mL, with a minimal volume of 500 µL, and filtered through a 40 µm sterile cell strainer (Thermo Fisher Scientific, 22-363-547) into 5 mL falcon round-bottom polystyrene tubes (Thermo Fisher Scientific, 14-959-2A) prior to

flow cytometry. GFP fluorescence was measured on BD FACSCelesta Flow Cytometer or BD LSRFortessa Cell Analyser which were calibrated with untransfected HEK 293A GFP and HEK 293T controls. Ten thousand events were counted. Kaluza Flow Cytometry Analysis Software was used to gate the cells in order to exclude debris and cell clumps from analysis. Knockdown efficiency was evaluated by geometric mean fluorescence intensity (Geo MFI) percentage in relation to control samples of cells transfected with the associated reagent and scramble siRNA concentration.

Small EV isolation

Cells were grown to 70-80% confluence. DMEM was removed, followed by a 1X PBS wash, to remove any remnants of contaminating small EVs originating from the FBS in the DMEM, then replaced with UltraCULTURE serum-free medium.

Differential centrifugation involved centrifuging the UltraCULTURE collected off cells or directly from the stock bottle at 300 xg (TX-400 rotor, Thermo Fisher Scientific) for 10 min to remove contaminating cells then decanting the supernatant and centrifuging it at 2,000 xg (TX-400 rotor, Thermo Fisher Scientific) for 10 min to remove contaminating dead cells. The supernatant was again decanted and centrifuged at 10,000 xg (F15-6x-100y rotor, Thermo Fisher Scientific) for 30 min to remove contaminating cell debris. The supernatant was then centrifuged at 28,500 rpm (100,000 xg) (SW 40 Ti, SW 41 Ti or SW 32 Ti Swinging-Bucket rotors, Beckman Coulter Life Sciences) in thick wall polycarbonate tubes (Beckman Coulter Life Sciences, 355631) for 2 hours. The pellet of small EVs was vigorously resuspended in 1 mL 1X PBS and re-centrifuged for a wash at 49,000 rpm (100,000 xg) (TLA-100.3 Fixed-Angle Rotor, Beckman Coulter Life Sciences) in polypropylene tubes (Beckman-Coulter Life Sciences,

357448) for 30 min. The re-pelleted small EVs were resuspended in 50 µL[1] 1X PBS and were analyzed and quantified using Nanoparticle Tracking Analysis (NTA) on a ZetaView PMX-110. Where described, treatment of the small EVs ensued prior to RNA isolation with 500 µL Trizol reagent (Thermo Fisher Scientific, 15596018).

Transfection complex isolation

The differential centrifugation protocol used for small EV isolation was scaled down using Beckman Coulter Life Sciences conversion calculator (https://www.mybeckman.ca/centrifuges/rotors/calculator) in order to perform the protocol with less transfection reagent. Transfection complexes were prepared following the manufacturer's protocol for a well of a 6-well plate (see above). RNAiMAX, INTERFERin and RiboJuice were complexed with GFP siRNA at a final concentration of 10 nM as if they were going to be transfected in a final volume of 2 mL. The same amount of GFP siRNA was electroporated in 200 µL Opti-MEM with the same settings mentioned previously. Following complexation, the transfection complexes and electroporated siRNA were transferred to 1mL 1X PBS for differential centrifugation since the small EV-like particles in UltraCULTURE would've masked the results. An equal amount of GFP siRNA was also added alone to 1X PBS as a control. The samples were centrifuged at 300 xg (FA-45-24-11 5424R, Eppendorf) for 2 min then the supernatant was decanted and centrifuged at 2,000 xg (FA-45-24-11 5424R, Eppendorf) for 2 min. The supernatant was again decanted and centrifuged at 15,000 rpm (10,000xg) (TLA-100.3 Fixed-Angle Rotor, Beckman Coulter Life Sciences) in polypropylene tubes for 5 min. The supernatant was then centrifuged at 49,000 rpm (100,000xg) (TLA-100.3 Fixed-Angle Rotor, Beckman Coulter Life Sciences) in polypropylene tubes for 30 min. The pellet was vigorously

[1] When small EVs were used to treat NHDF-Neo, they were resuspended in 10 µL instead

resuspended in 1 mL 1X PBS and re-centrifuged at 49,000 rpm (100,000xg) (TLA-100.3 Fixed-Angle Rotor, Beckman Coulter Life Sciences) in polypropylene tubes for another 30 min. The re-pelleted small EV-like particles were either resuspended in 50 µL 1X PBS and analyzed and quantified using Nanoparticle Tracking Analysis (NTA) on the ZetaView or were combined with 500 µL Trizol reagent for RNA isolation.

Nanoparticle tracking analysis

Nanoparticle Tracking Analysis (NTA) was performed on a ZetaView PMX-110. The ZetaView was calibrated upon each start-up using 102 nm polystyrene beads (Microtrac, 900383). Transfection complexes or precipitated small EVs were diluted in 1X PBS (1,000X-1,000,000X) to be in the instrument's range for accurate measurement. Approximately 700 µL of the dilution was injected into the instrument. Once particle drift and concentration fell in acceptable ranges, video acquisition was performed with the following settings: Sensitivity 85, Shutter Speed 40, Frame Rate (fps) 30, Resolution Highest, Camera Gain 770, Positions Measured 11, Minimum Brightness 15, Minimum Size (pixels) 10, Maximum Size (pixels) 500. The resulting analysis reported the particle size distribution, the median particle size, and the concentration of the original undiluted sample taking into account the dilution factor. The Gibbings lab has validated NTA with 110 nm polystyrene beads of known concentration (Microtrac, 400168).

RNase & detergent treatments

Treatment of small EVs

Equal amounts of the small EVs' resuspension in 1X PBS, was divided into 3; untreated, treated with RNase A, and treated with RNase A + detergent. Where described, detergent (0.5% SDS, 0.5% triton X-100) was added. 1X PBS was also added so that all 3 samples resulted in equal volumes once the RNase was added. Immediately after addition of 5 µg RNase A (Thermo

Fisher-Scientific EN0531 or Qiagen, 19101), samples were incubated for 10 min at 37°C on a shaking heat block. Five hundred microliters of Trizol reagent was hastily added to halt the reaction after the incubation period for RNA isolation.

Treatment of transfection complexes

Transfection complexes were formed as described above but using the amounts recommended for a well of a 24-well plate and a final GFP siRNA concentration of 10 nM in 500 µL: RNAiMAX (25 µL X2 Opti-MEM + 5 µL 1000 nM siRNA + 1.5 µL RNAiMAX), INTERFERin (100 µL Opti-MEM + 5 µL 1000 nM siRNA + 2 µL INTERFERin), and RiboJuice (48 µL Opti-MEM + 5 µL 1000 nM siRNA + 2 µL RiboJuice). Equivalent amounts of GFP siRNA were electroporated in 100 µL Opti-MEM with the parameters mentioned above and equivalent amounts of GFP siRNA alone in 100 µL Opti-MEM controlled for functioning of the RNase. After the complex incubation times recommended by the manufacturers, each sample was divided into 3; as mentioned above. Detergent was added to appropriate samples and samples were topped with nuclease-free water for the 3 samples to have equal volumes after the addition of RNase A which occurred right before incubation on a shaking heat block at 37°C for 10 min, immediately followed by the addition of 500 µL of Trizol reagent.

RNA isolation

A standard Trizol extraction protocol was followed. This involved mixing 0.2 mL of chloroform (Thermo Fisher Scientific, BP1145-1) per mL of Trizol reagent and incubating at room temperature 15 min, then centrifuging at 12,000 xg for 15 min at 4°C. The aqueous phase was combined with 10 µg of glycogen (Thermo-Fisher Scientific, R0551 or AM9515) and isopropanol (0.5 mL per mL of Trizol reagent). The RNA was precipitated at 13,500 rpm for 30 min at 4°C. The resulting pellet was washed with 75% nuclease-free ethanol (1 mL per mL of Trizol reagent) and centrifuged at 13,500 rpm for 30 min at 4°C. The dry RNA pellet was then

resuspended in 20 µL of nuclease-free water. Quantification and analysis was completed with Nanodrop 2000 spectrophotometer (Thermo Fisher Scientific, ND-2000) or a Synergy H1 Hybrid Multi-Mode plate reader (BioTek).

Northern Blot

55 µg of RNA collected from NSC-34 cells transfected with modified and unmodified SOD1-tageting RNA was combined with 2X RNA loading dye (Thermo Fisher Scientific, R0641) and heated at 80°C for 5 min, then incubated on ice 5-10 min prior to loading on a pre-ran 17.5% polyacrylamide (40% bis-acrylamide 19:1 solution) (Thermo Fisher Scientific, BP1406-1) 7 M urea gel (Thermo Fisher Scientifc, BP169-212). RNA separation occurred in 0.5X TBE (Wisent Bioproducts, 880-545-CL) alongside 1 µL microRNA marker (NEB, N2102S) for 30 min at 150V then 250V. The RNA was transferred to a positively charged nylon membrane (Millipore Sigma, 1417240) using a Trans-Blot Turbo Transfer System (Bio-Rad, 1704150) for 90 min at 0.2A 25V also in 0.5X TBE. The RNA was UV crosslinked to the membrane with a Stratalinker 2400, delivering 120 mJ to each side of the membrane twice.

18 pmol custom DNA oligonucleotide probes for SOD1-targeting RNA (IDT, 5'AAGCATTAAAGGACTGACTGAA3') was labeled with 30 µCi of ATP[γ-^{32}P] (PerkinElmer, BLU002A500UC) using 10U T4 PNK (NEB, M0201S) during an hour incubation at 37°C followed by heat inactivation at 68°C for 10 min. The labeled probe was separated from unincorporated nucleotides by ethanol precipitation which involved adding the following and incubating at -80°C for at least 20 min: 10 µg glycogen, 180 µl 1X TE buffer, 20 µl 3M sodium acetate (pH5.5) and 800 µL 100% EtOH. This was then centrifuged at 13,500 rpm for 30 min at 4°C and the pellet was washed with 1 mL 75% EtOH then re-centrifuged at 13,500 rpm for 5 min at 4°C. The dried pellet was resuspended in 50 µL 1X TE.

The membranes were pre-hybridized in 10 mL of PerfectHyb Plus Hybridization buffer (Sigma, H7033) for 1 hour at 40°C and hybridized with labeled probe overnight under the same conditions. Membranes were washed twice with 20 mL 5X SSC + 0.1% SDS for 20 min and once with 20 mL 1X SSC + 0.1% SDS for 20 min before exposure to storage phosphor screens (GE Healthcare). Screens were imaged using a Typhoon Trio machine (GE Healthcare).

RT-qPCR

Quantification of SOD1-targeting RNA constructs

MiScript II RT kit (Qiagen, 218161) and Custom Taqman Small RNA Assay (Thermo Fisher Scientific, 4398988) were used to reverse transcribe an equal amount of SOD1 targeting RNAs (6.25 fmol). The manufacturer's miScript PCR system handbook was followed with the HiFlex buffer option but with 0.5 µL miScript Reverse Transcriptase Mix in a 20 µL reaction. For TaqMan Small RNA Assay, denaturing the siRNA template with custom sequence-specific RT primers for SOD1-targeting RNA was recommended by the manufacturer's Taqman Small RNA Assay protocol prior to performing the reverse transcription reaction. The reverse transcription protocol ensued with 50U M-Mulv Reverse Transcriptase (NEB, M0253L) in a 10 µL reaction.

Following miScript II RT, cDNA (1 µL 1:6) was amplified using the miScript SYBR Green PCR kit (Qiagen, 218076) and 10X miScript SOD1 primer assay (5µM) (IDT, 5'TTCAGTCAGTCCTTTAATGCTT3') in accordance with the manufacturer's miScript PCR system handbook on a CFX384 or CFX96 Touch Real-Time PCR Detection System (Bio-Rad, 1855485 or 1855195) using a 10 µL reaction volume. Following Custom Taqman Small RNA Assay, cDNA (2 µL 1:4) was amplified with TaqMan Gene Expression Master Mix (Thermo Fisher Scientific, 4369510), custom SOD1 primers/probe (20X) in accordance with the manufacturer's Taqman Small RNA Assay protocol and the following thermal cycler protocol:

95°C 4 min followed by 50 cycles of 95°C 15 sec and 60°C 40 sec. The C_q values were made relative to the unmodified ssRNA which amplified the best.

Quantification of transfected SOD1-targeting RNA

One hundred nanograms of RNA isolated from cells transfected with SOD1-targeting RNA and the resulting small EVs was added to Custom Taqman Small RNA Assay following the protocol described above. qPCR was performed simultaneously on samples and a serial dilution of a known amount (6.25 fmol) of unmodified ssRNA reverse transcribed with Custom Taqman Small RNA Assay to generate a standard curve. C_q values of samples were correlated to the number of RNA molecules in the reverse transcription reaction using the standard curve. As the RNA was prepared from a known number of small EVs (determined by NTA), the number of RNA molecules per sEV was calculated.

Quantification of transfected GFP siRNA and transfection complexes

An equal volume (6.5 µL) of RNA isolated from treated sEVs originating from cells transfected with GFP siRNA or precipitated transfection complexes was reverse transcribed using the miScript II RT kit as described above but using the HiSpec buffer option and 0.5 µL miScript Reverse Transcriptase Mix in a 10 µL reaction. A known amount of GFP siRNA (13 fmol) was also reverse transcribed to generate a standard curve during the qPCR using miScript SYBR Green PCR kit as described above with the GFP siRNA primer (5' ATGAACTTCAGGGTCAGCTTGC 3').

GFP siRNA primer annealing temperature was tested on pooled cDNA samples of transfection complexes and pooled samples of HEK 293T small EVs to ensure that the annealing temperature recommended by the manufacturer's protocol was in the primer's range of efficiency. Additionally, amplification of a serial dilution of these pooled samples helped

determine the level of dilution (1:100) the cDNA should be diluted to be within the primer's efficiency range for qPCR. These steps are in accordance with MIQE guidelines.

Treatment of GFP NHDF-Neo with small EVs

Five hundred NHDF-Neo expressing GFP were seeded per well of an imager quality 384 well plate (Aurora Microplates, ABC201201A) in 40 µL of culture media. Twenty hours later, $5x10^8$ small EVs isolated from HEK 293T, HEK 293T expressing GFP siRNA or HEK 293T expressing GFP siRNA transfected with scramble siRNA were added on the NHDF-Neo cells (~500,000 particles/cell). Three days post-treatment, GFP knockdown was quantified by Opera Phenix High-Content Screening System (PerkinElmer, HH14000000) in the High Throughput Screening Lab at CHEO Research Institute. Image analysis was performed using Columbus Image Data Storage and Analysis System (PerkinElmer). Nine fields containing a total of at least 100 cells were analyzed. The GFP region of each field was selected automatically by lowering the automatic threshold as low as possible while still discriminating between cell body and background, and GFP mean intensity was measured in a batch analysis. Knockdown is presented as a percent reduction in GFP mean fluorescence intensity compared to wells that received small EVs originating from HEK 293T.

CD63 staining

Cover slips were washed twice with 1X PBS then incubated with 300 µL purified mouse anti-human CD63 antibody (1:100) (BD Pharmingen, 556019) in 1% BSA 0.25% Triton X-100 in 1X PBS overnight at 4°C in the dark. The following day, the cover slips were washed twice with 1X PBS then incubated with 300 µL goat anti-mouse Alexa 488 (1:500)(Thermo Fisher Scientific, A11029) in 1% BSA 0.25% Triton X-100 in 1X PBS for 1 h at 4°C. Then, cover slips were washed twice with 1X PBS and mounted with VECTASHEILD solution (Vector

Laboratories Inc, H-1200) and sealed with nail polish. Unstained transfected cells as well as stained untransfected cells acted as controls. Additional controls included staining with primary or secondary antibodies only. Images were acquired by confocal microscopy (ZEISS Axio Imager 2, CBIA Core, University of Ottawa) with a 63X Plan-Apochromat 1.4 Oil lens and the ZEN 2.3 analysis software.

Statistical Analysis

Statistical analysis was performed with using GraphPad Prism 7 software.

Results

TaqMan Small RNA Assay better quantifies chemically modified RNA

Quantification of chemically modified RNA using miScript II RT-qPCR

Three different small RNAs targeting SOD1 are used for the purposes of this project; a single stranded (ss) 22 nt RNA which mimics the guide strand of SOD1 siRNA, a double stranded (ds) SOD1 siRNA and the same SOD1 targeting sequence integrated in a 42 nt pre-miR-451 hairpin backbone (**Figure 5c**). The three forms each have a version made exclusively of unmodified ribonucleosides and a version modified with stabilizing chemistries. These modifications include 2'-O-methyl and 2'fluoro nucleosides as well as phosphorothioate bonds that link the nucleosides together instead of the usual phosphodiester bonds. Modifications in the 42 nt hairpin RNA are lacking from nt 23 to 32 to allow for its usual processing by Ago2 and exonucleases.

In order to measure the packaging of these RNAs in small extracellular vesicles (sEVs), it was first verified that a method is able to equivalently quantify these. The RNAs possess an identical sequence which was targeted for comparison. According to absorbance at 260 nm, equal amounts of modified and unmodified ssRNA and hairpin RNA were added to RT-qPCR reactions using the miScript II RT kit. This method involves polyadenylating the RNA to then initiate cDNA synthesis through the annealing of oligo-dT primers (**Figure 5a**). The modified ssRNA was detected 10 quantitation cycles (C_q) later than its unmodified counterpart (**Figure 5d**). This suggests that the capacity to detect chemically stabilized RNAs with the miScript II RT-qPCR kit is impaired. With this RT-qPCR method, quantities of modified ssRNA are inaccurately read as 300-6,000 fold lower than similar amounts of unmodified ssRNA. Similarly, both the unmodified and modified hairpin RNAs were detected 12 C_q later than the unmodified

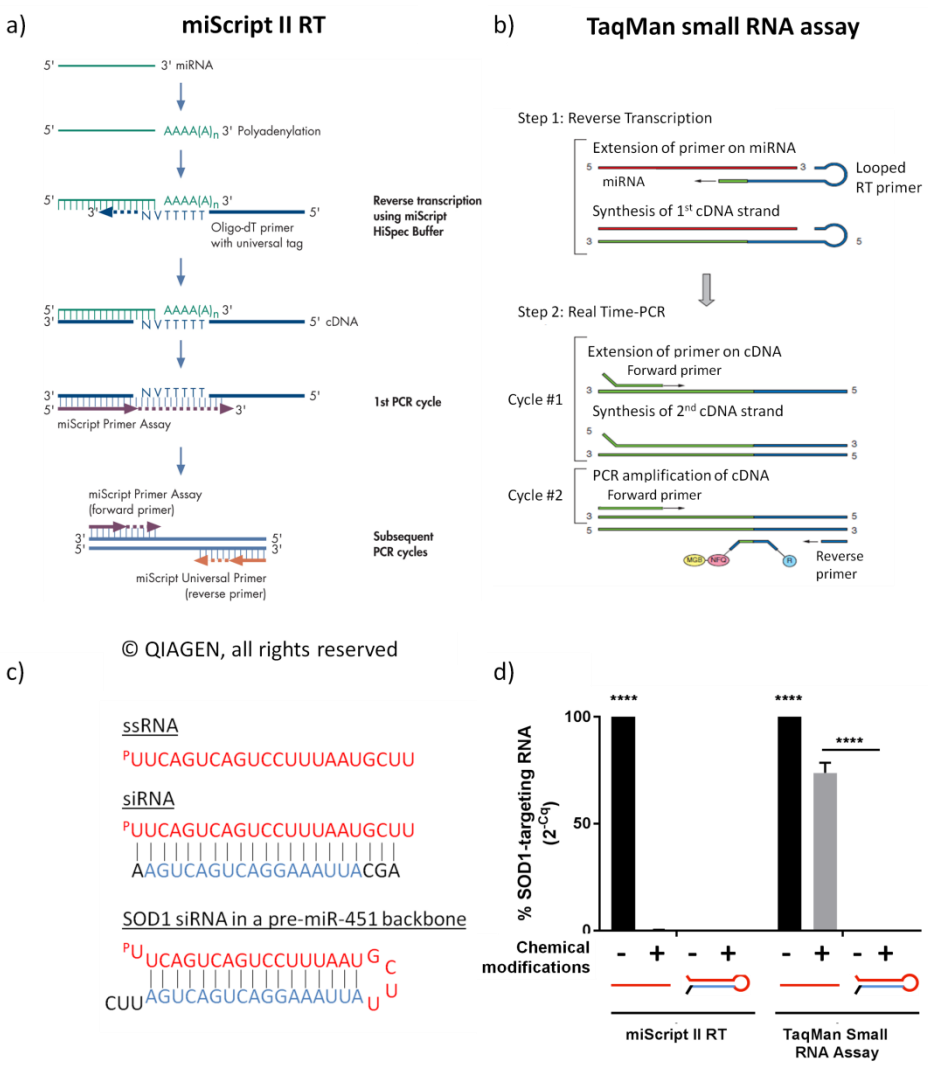

FIGURE 5. Impact of SOD1-targeting RNA's chemical modifications on quantification by RT-qPCR. Mechanism of (a) Miscript II RT-qPCR and (b) TaqMan Small RNA Assay. (Reprinted with permission from QIAGEN and ThermoFisher Scientific). (c) Structure of SOD1-targeting RNAs. P, phosphate; ss, single stranded (d) An equal amount of modified or unmodified hairpin and single stranded(ss) RNA are quantified by RT-qPCR with either method. The relative quantity is determined through $2^{(-Cq)}$ and made relative to the unmodified ssRNA. (n=2) Statistics: Two-way ANOVA Sidak's multiple comparisons test.

ssRNA, suggesting the hairpin structure also impairs RT-qPCR. In sum, miScript II RT-qPCR did not accurately measure the SOD1-targeting small RNAs and had a large bias towards unmodified ssRNA potentially due to its lack of secondary structures and chemical enhancements.

Quantification of chemically modified RNA using TaqMan Small RNA Assay

TaqMan Small RNA Assay uses a different mechanism than miScript II RT-qPCR (**Figure 5b**). It does not have a polyadenylation step and instead uses custom hairpin primers to synthesize cDNA. Therefore, quantification of modified RNAs may be more accurate. Again, according to A_{260}, equal amounts of modified and unmodified ssRNA and hairpin RNA were subjected to RT-qPCR with Taqman Small RNA Assay. This kit revealed less than 0.5 C_q difference (1.5-fold difference) when equal amounts of modified and unmodified ssRNA were quantified (**Figure 5d**). Therefore, TaqMan Small RNA Assay is much more accurate in quantifying ssRNA having or lacking chemical enhancements compared to miScript II RT-qPCR. However, TaqMan Small RNA Assay did not improve the detection of the hairpin RNA. In conclusion, TaqMan Small RNA appears to be the most accurate means available to quantify SOD1-targeting RNA in transfected cells and their small EVs.

Packaging chemically enhanced SOD1-targeting RNAs in small EVs

Chemical modifications do not prevent pre-miR-451 maturation

The pre-miR-451 RNA is known to be processed in a Dicer-independent manner. A northern blot of transfected NSC-34 cells was performed to demonstrate the maturation of the 42 nt pre-miR-451 hairpin structure containing the SOD1 siRNA sequence into a ~22 nt RNA. The results revealed the presence of variously sized bands suggesting that part of this hairpin is processed in the cells to produce the mature SOD1 siRNA (**Figure 6a**). The band located higher

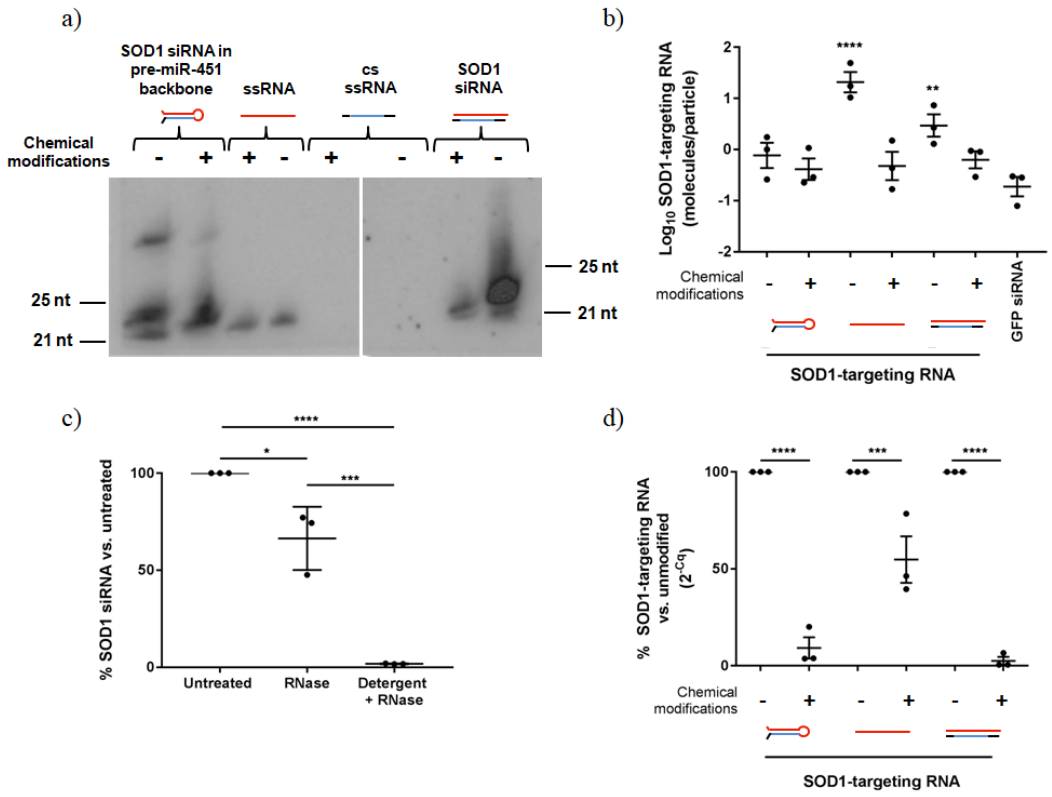

FIGURE 6. Packaging various SOD1-targeting RNAs into small EVs. (a) Northern blot of RNA isolated from cells transfected with various small RNAs. ss, single stranded; cs, complementary strand; ds, double stranded. (b) Absolute copy number of SOD1-targeting small RNAs per sEV released by NSC-34 cells transfected with the various RNAs. (n=3) Statistics: One-way ANOVA Dunnett's multiple comparisons test in relation to GFP siRNA. (c) Absolute copy number of SOD1 siRNA in RNase +/- detergent-treated sEVs originating from cells transfected with unmodified SOD1 siRNA relative to copies in untreated sEVs. (n=3) Statistics: One-way ANOVA Tukey's multiple comparisons test. (d) Relative quantity of modified RNAs in transfected cells relative to the quantity in cells transfected with the unmodified counterpart. (n=3) Statistics: One-way ANOVA Sidak's multiple comparisons test.

than the miRNA marker could represent the full 42 nt hairpin or the fragment resulting from cleavage by Ago2. We also saw two fragments near 22 nt. One could represent the mature siRNA and the slightly larger could represent the form being progressively trimmed by exonucleases to form the mature siRNA. Similar processing was observed when cells were transfected with a similar hairpin RNA containing chemical modifications. These modifications were not located where the exonucleases would trim the Ago2-cleaved pre-miRNA. Therefore, it can only be said that these modifications did not seem to prevent cleavage by Ago2. As small amounts of RNA were isolated from the small extracellular vesicles (sEVs) produced by the transfected cells, the SOD1-targeting RNAs were not detected by northern blot. This would have validated which forms were loaded in the sEVs. However, Reshke et al. demonstrated that the sEVs, collected from stable cells expressing the recoded pre-miR-451, carried both the mature siRNA and hairpin form[20]. In conclusion, the hairpin RNA matured to form the SOD1 siRNA. TaqMan Small RNA Assay would not be able to distinguish between these forms. However, the linear SOD1 siRNA is the form better detected by RT-qPCR.

Unmodified RNAs have higher copy number in small EVs

NSC-34 cells were transfected with the various SOD1-targeting RNAs to test whether modified RNAs could be loaded into small EVs (sEVs) by transfection of sEV-producing cells. The sEVs, collected from transfected cells, were in the size range described for exosomes and smaller microvesicles (< 200 nm).

The SOD1-targeting RNA in these sEVs was quantified by TaqMan Small RNA Assay RT-qPCR. A standard curve of known amounts of ssRNA was used to determine the absolute copy number in the RT-qPCR. Since the RNA was extracted from a known number of sEVs, counted by nanoparticle tracking analysis, we determined the amount of copies per sEV. The SOD1-targeting RNA level in sEVs originating from cells transfected with the unmodified

siRNA was consistently higher than the background level established by transfection with GFP siRNA. These sEVs had 25 copies per sEV (**Figure 6b**). sEVs produced by unmodified ssRNA-transfected cells also had a copy number higher than background level, with nearly four copies per sEV. The other SOD1-targeting RNAs in sEVs were comparable to background levels.

In order to confirm that these copies were located within the sEVs, RNase treatments were applied in the presence or absence of detergent. Detergent would disrupt the sEVs' membrane leading to digestion of the small RNAs enclosed within them. However, an RNase treatment without detergent would only be able to digest the RNA that is located outside of the sEVs. These treatments were compared to the untreated sEVs to reveal the percentage of RNA located inside them. The sEVs which had a copy number of 25 small RNAs per sEV (unmodified siRNA) were RNase treated. An average of 66% of the SOD1 siRNA was protected from the RNase and thus, was suspected to be inside the sEVs, while only 1.75% remained when detergent was introduced prior to the RNase (**Figure 6c**). The unprotected 33% could signify that some of the sEV membranes were compromised by the isolation and storage protocol. However, it is also possible that the siRNA was attached on the outside surface of the sEVs or released as free siRNA. This may mean that the copy number is overestimated and more like 16 per sEV. Also, there may be a difference in internal packaging into sEVs between the sEVs collected from SOD1 siRNA-transfected cells and the ssRNA-transfected cells. In conclusion, cells transfected with siRNA do not release all transfected siRNA through sEVs and these levels may vary between RNAs.

Unmodified RNAs have higher levels in transfected cells than modified RNAs

Low levels of the small RNAs in sEVs may be caused by low levels in the transfected cells. Indeed, the levels of SOD1-targeting small RNAs in cells paralleled closely their respective levels in small EVs. Additionally, small RNA levels in cells transfected with all

unmodified versions was higher than in cells transfected with the modified equivalent (**Figure 6d**). This parallels with the unmodified ssRNA and double stranded forms having higher levels in sEVs than the chemically stabilized RNAs. In conclusion, levels in the cells transfected with unmodified versions of single stranded and dsRNA correlate with levels in sEVs.

The results suggest that the modified forms struggle to be internalized by cells or stay in the cells. Although not demonstrated here, modifications increase the stability of RNA[6,7]. Therefore, if RNA degradation was the primary force determining the level of RNAs in the cell, the modified RNAs should have higher levels in cells compared to unmodified RNA, but the opposite was observed. This could mean that the modified RNAs were struggling to form transfection complexes or be internalized by cells. We speculate that the chemical modifications or secondary structures hinder interactions with the transfection reagents or assembly of transfection complexes thus, resulting in varying transfection efficiencies. This could explain why the unmodified single stranded and dsSOD1-targeting RNAs had higher levels in cells and in sEVs. Identifying a reagent or method that efficiently transfects modified RNAs into cells may improve its packaging into sEVs for therapeutic use.

Highest siRNA concentration produces optimal transfection with various methods

As mentioned above, the levels of small RNAs in small EVs (sEVs) correlated with levels in the transfected sEV-producing cells. Additionally, chemically modified RNA did not seem to transfect as efficiently. Therefore, transfection conditions and timing that provides the maximum knockdown of a target mRNA in cells, may indicate the maximum availability of RNAs in the cytoplasm for packaging into sEVs. Optimizing transfection to increase the efficiency of internalization of chemically modified small RNAs may in turn support their packaging into sEVs. Three chemical transfection methods (RNAiMAX, INTERFERin and

RiboJuice) and one physical transfection method (electroporation) were compared. All three reagents are cationic suggesting they interact with nucleic acids and cellular membrane in related ways. However, as their components are different, details of their complex formation, their uptake and endosome escape may vary. On the other hand, electroporation bypasses these steps by directly introducing the RNA into the cytoplasm through pores in the plasma membrane made with an electric field and thus may lead to more RNA available for packaging into sEVs. As GFP knockdown is measurable by flow cytometry, optimization was performed using a GFP siRNA transfected into GFP-expressing HEK 293A. To select the optimal conditions for each transfection method, multiple time points and siRNA concentrations were screened using the manufacturer's recommended conditions.

Transfection without reagents (siRNA only) did not produce a knockdown effect (**Supplementary 1a**) and no significant differences were observed in the mean fluorescence of untransfected cells and cells transfected with the scramble siRNA and the various reagents/electroporation (**Supplementary 1b, 2b**). Additionally, knockdown was not significantly different whether electroporation cuvettes were re-used versus brand new (**Supplementary 2a**). In conclusion, siRNA is unable to be internalized without reagents or electroporation and untransfected cells are equivalent to cells transfected with control siRNA.

Although not significant, knockdown with the three transfection reagents seemed stronger at three days after transfection as compared to their effects at two days (**Figure 7**). In comparison, electroporation demonstrated a higher knockdown after two days, most likely due to the direct introduction of the siRNA into the cytoplasm with this method (**Figure 7a**). While knockdown tended to increase with increasing doses of siRNA, a plateau was reached at a dose of 5-10 nM. It is possible that the transfection reagent is saturating leading to a maximum

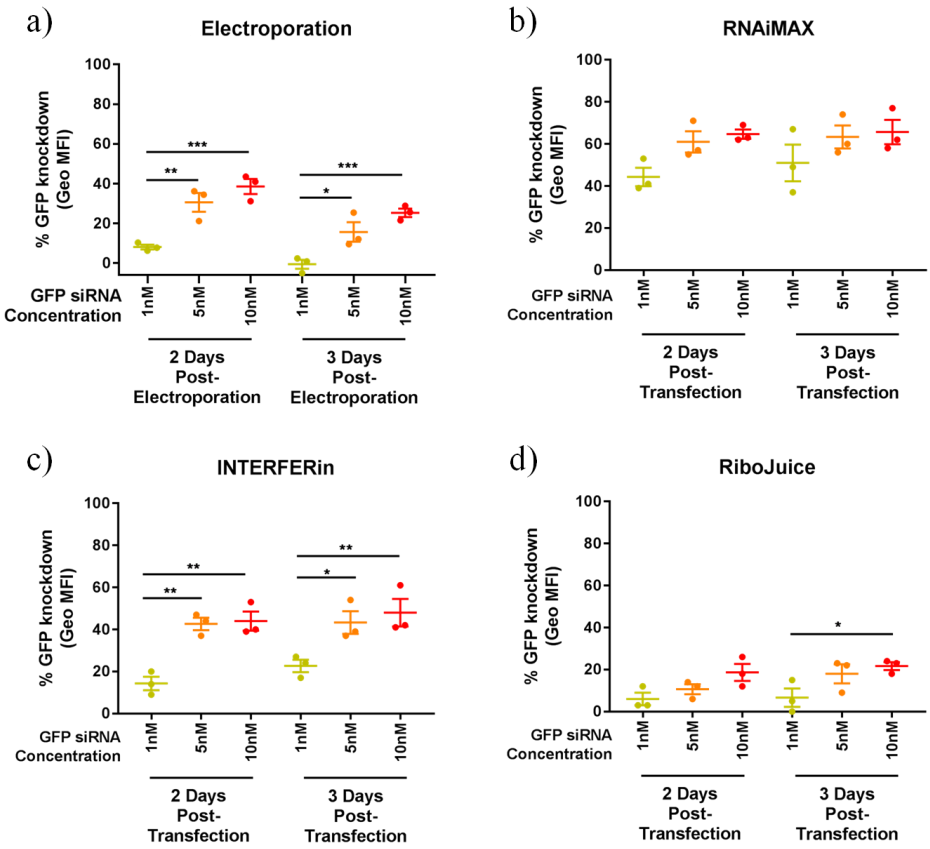

FIGURE 7. Relative GFP knockdown in cells transfected with GFP siRNA using various transfection methods. Flow cytometry measured GFP fluorescence in HEK 293A GFP cells two or three days after transfection using (a) electroporation (n=3), (b) RNAiMAX (n=3), (c) INTERFERin (n=3), and (d) RiboJuice (n=3). Geometric mean fluorescence intensity (Geo-MFI) was normalized to samples transfected with control siRNA at the associated concentration and with the associated reagent. Statistics: Two-way ANOVA Tukey's multiple comparisons test.

amount of siRNA which can enter the cells thus resulting in the start of a plateau for GFP knockdown. Alternatively, if the plateau is caused instead by saturation of siRNA, the higher concentration of 10 nM would provide more siRNA in the cytoplasm for packaging into sEVs. The 10 nM siRNA concentration was thus selected for subsequent experiments. In summary, all transfection methods had best knockdown with the 10 nM siRNA concentration; three days post-transfection for the reagents and two days post-transfection for electroporation. Maximum knockdown was obtained with RNAiMAX (66%, **Figure 7b**) followed by INTERFERin (48%, **Figure 7c**), electroporation (39%, **Figure 7a**) and RiboJuice (18%, **Figure 7d**).

GFP siRNA is detected in sEV preparations after transfection with electroporation, RNAiMAX and INTERFERin

The optimal conditions, for delivery of siRNA into the cells' cytoplasm with each transfection method, were used to determine the method which packages the most GFP siRNA into small EVs. Standard culture media containing FBS is rich in bovine sEVs which would contaminate the sEV preparations. Therefore, culture media was changed to serum-free ultraCULTURE media after transfection. Additionally, this media change removes transfection complexes that have not attached to cells or been internalized. Since it is unknown how long it takes for transfected siRNA to be packaged and released with sEVs, we aimed to start collection of sEVs as soon after transfection as possible. Therefore, GFP knockdown was compared between RNAiMAX/GFP siRNA-transfected cells which received a media change 6h after transfection and 24h after transfection. GFP knockdown in sEV-producing cells was similar whether media was replaced 6h or 24h after transfection, suggesting that transfection complex uptake is maximal already at 6h, and sEV collection can begin at this point (**supplementary 1c**).

To compare packaging of the GFP siRNAs into sEVs, UltraCULTURE was collected 24h, 48h and 72h post-transfection and pooled for sEV isolation. Transfection of cells with

RNAiMAX resulted in the maximum amount of siRNA in sEVs with 1 copy per 7 sEV (**Figure 8a**). This may correlate with transfection efficiency as RNAiMAX gave the best transfection efficiency. Introduction of siRNA into cells with electroporation or INTERFERin resulted in packaging of siRNA into sEVs at 1 copy per 15 sEV and 1 copy per 142 sEV respectively. No siRNA was detected in sEVs after transfection of cells with RiboJuice; comparable to untransfected cells. This is not surprising as RiboJuice had the worst transfection efficiency. In conclusion, the results support that transfection efficiency correlates with the amount of small RNA packaged into sEVs.

The sEVs produced from cells transfected with each method were treated with RNase to determine if the GFP siRNA copies were protected potentially inside sEVs. Sixty percent of GFP siRNA copies were protected when sEVs originated from electroporated cells (**Figure 8b**). However, a similar amount of the RNA was protected with a prior treatment of detergent. It is possible this siRNA is released in protein complexes which are more resistant to detergent. Small EVs released from RNAiMAX-transfected cells protected 45% of the siRNA from RNase (**Figure 8c**) whereas for INTERFERin-transfected cells only 12% was detected in the presence of RNase (**Figure 8d**). No RNA copies were detected in the presence of detergent for sEVs from RNAiMAX- and INTERFERin-transfected cells. In brief, this suggests the fate of the transfected siRNA is different according to the reagent used, where RNAiMAX seem to promote the release of more protected siRNA.

The copies of siRNA added to cells in transfection complexes was compared to the copies detected in the untreated sEVs to determine the percentage of packaged siRNA. Much less than 1% of transfected siRNA is released with sEVs (**Figure 8e**). Loss can be due to copies not entering the cells or not escaping the endosome and thus fusing with lysosomes and/or

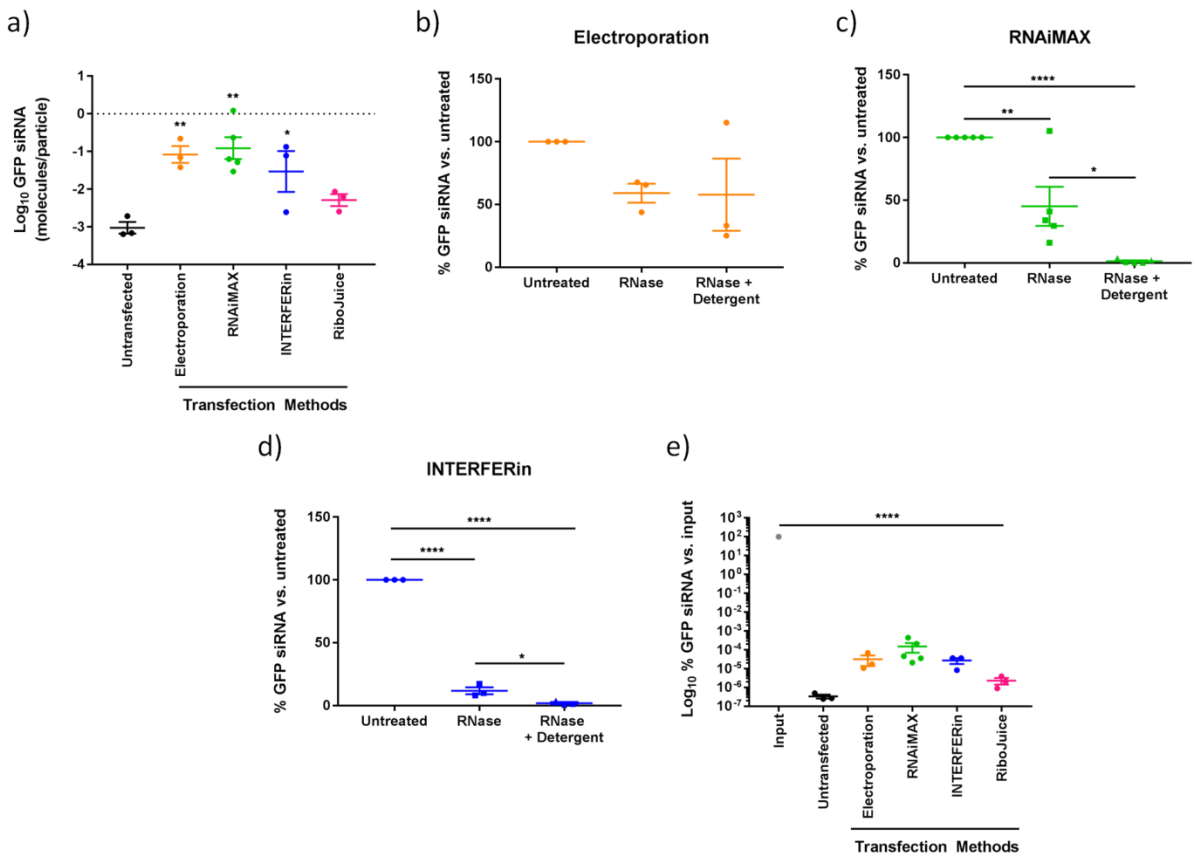

FIGURE 8. Packaging GFP siRNA into small EVs using the optimized transfection concentration of 10 nM. (a) Absolute copy number of GFP siRNA per sEV released by HEK 293T cells transfected with various transfection methods. Statistics: One-way ANOVA Dunnett's multiple comparisons test in relation to copy number in small EVs produced by untransfected cells (n=3). (b-d) Absolute GFP siRNA copies in RNase +/- detergent-treated small EVs originating from HEK 293T cells transfected using (b) electroporation (n=3), (c) RNAiMAX (n=5), or (d) INTERFERin (n=3), relative to copies in untreated sEVs. Statistics: One-way ANOVA Tukey's multiple comparisons test. (e) Absolute copies of GFP siRNA in sEVs released by HEK 293T cells transfected with various transfection methods relative to copies initially transfected. One-way ANOVA Dunnett's multiple comparisons test in relation to input.

getting exocytosed or simply not entering the sEVs packaging pathway. Additionally, the poor recovery of sEVs through differential centrifugation and RNA from Trizol extractions (demonstrated later in **Figure 11f**) can cause an underrepresentation of siRNA released with sEV. In sum, only a fraction of the initial amount of RNA transfected into cells is released and collected from the sEV isolations.

Transfection complexes versus small EVs

Transfection complexes may be co-localizing with the late endosome

Transfection complexes have previously been observed to accumulate in late endosomes[17]. Small EVs, specifically exosomes, are produced by the inward budding of late endosomes. Therefore, as the exosomes and transfection complexes share this compartment, fusion of late endosome with the plasma membrane could lead to release of both. This would mean that sEV preparations could contain transfection complexes and these transfection complexes could influence sEV copy number and siRNA delivery. It is also a possibility that transfection complexes would fuse with sEVs.

Microscopy was used to demonstrate that a fluorescently-tagged siRNA co-localized with CD63, a late endosome and exosome marker, even two days after transfection with RNAiMAX (**Figure 9**). Therefore, transfection complexes as a whole may co-localize with the endosome and release with sEVs after transfection and thus contaminate sEV preparations.

Transfection complexes co-precipitate with sEVs

If transfection complexes are released with small EVs, would they be distinguishable by nanoparticle tracking analysis (NTA)? To test this, transfection complexes were made with the different reagents and GFP siRNA then analyzed by NTA. The results demonstrated that there

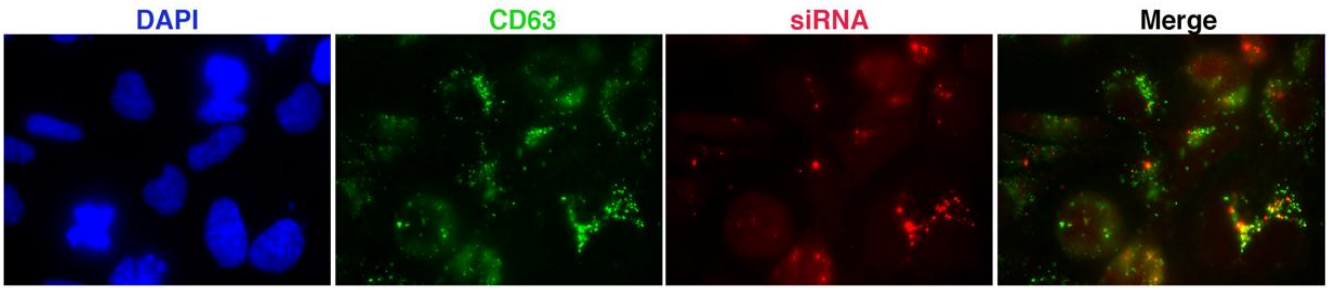

FIGURE 9. Transfected siRNA co-localizes with the late endosome marker CD63 by fluorescent microscopy. HEK 293T cells were transfected with RNAiMAX and a fluorescently labeled siRNA. Two days after transfection the cells were fixed and stained for CD63.

were no significant differences observed in the median sizes between transfection complexes and the sEVs (**Figure 10a**). Of note, transfection reagents without siRNA also exhibited a similar median size to sEVs and transfection reagents complexed with siRNA (**supplementary 4**). This suggests that siRNA does not drastically increase the size of the transfection complexes. However, a closer evaluation of the size distributions of transfection complexes, sEVs and reagents may reveal differences.

The median sizes of transfection complexes are undistinguishable from sEVs suggesting they may pellet with sEVs during differential centrifugation. Thus, the transfection complexes were subjected to the sEV isolation protocol to test if they would be purified with sEVs, if released alongside them by transfected cells. Transfection complexes persisted after the sEV preparation protocol. However, sEV-sized particles were only detectable once after differential centrifugation of GFP siRNA alone and RiboJuice transfection complexes. Again the median sizes were similar to the sEVs (**Figure 10b**). However, comparing size distribution profiles revealed differences between the differentially centrifuged INTERFERin-siRNA complexes or electroporated siRNA and the HEK 293T sEVs. Compared to sEVs produced by HEK 293T cells, the differentially centrifuged INTERFERin-siRNA complexes or electroporated siRNA had a decreased amount of particles in the 105 nm size range (**Figure 10d,f**). Differentially centrifuged RNAiMAX transfection complexes, on the other hand, did not differ from the HEK sEVs' size distribution profile (**Figure 10e**). Therefore, if these RNAiMAX transfection complexes are present in sEV preparations, they cannot be differentiated from sEVs by NTA. Differentially centrifuged GFP siRNA alone and Ribojuice-RNA complexes both revealed peaks in small size ranges (45-75 nm). Overall, nanoparticle tracking analysis was able to detect sEV-sized particles after differentially centrifuging transfections complexes and distribution profiles,

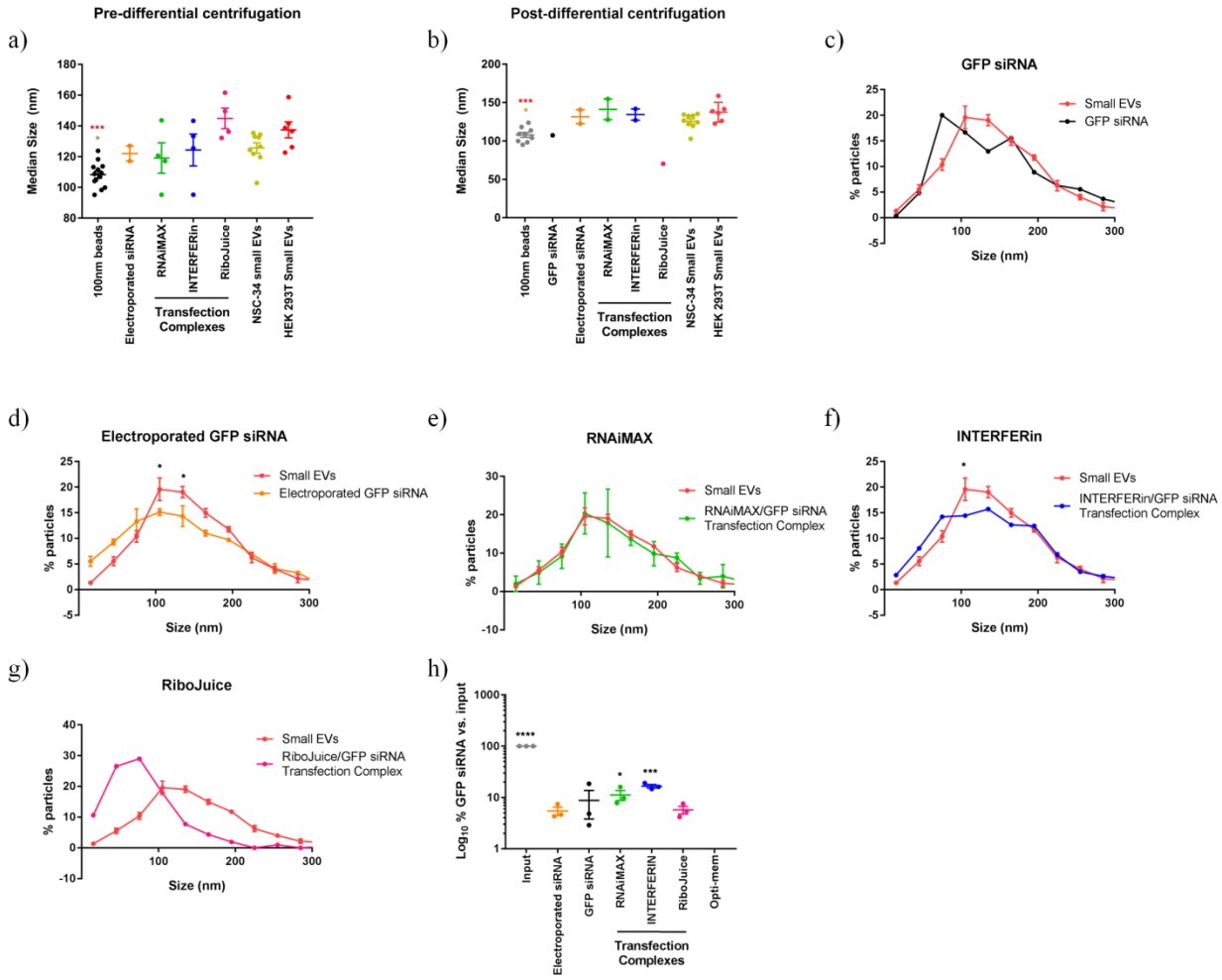
a)
Pre-differential centrifugation
Median Size (nm)
100nm beads
Electroporated siRNA
RNAiMAX
INTERFERin
RiboJuice
Transfection Complexes
NSC-34 small EVs
HEK 293T Small EVs
b)
Post-differential centrifugation
Median Size (nm)
100nm beads
GFP siRNA
Electroporated siRNA
RNAiMAX
INTERFERin
RiboJuice
Transfection Complexes
NSC-34 Small EVs
HEK 293T Small EVs
c)
GFP siRNA
Small EVs
GFP siRNA
% particles
Size (nm)
d)
Electroporated GFP siRNA
Small EVs
Electroporated GFP siRNA
% particles
Size (nm)
e)
RNAiMAX
Small EVs
RNAiMAX/GFP siRNA Transfection Complex
% particles
Size (nm)
f)
INTERFERin
Small EVs
INTERFERin/GFP siRNA Transfection Complex
% particles
Size (nm)
g)
RiboJuice
Small EVs
RiboJuice/GFP siRNA Transfection Complex
% particles
Size (nm)
h)
Log10 % GFP siRNA vs. input
Input
Electroporated siRNA
GFP siRNA
RNAiMAX
INTERFERIN
RiboJuice
Opti-mem
Transfection Complexes

FIGURE 10. siRNA transfection complexes are retrieved by standard protocols for preparation of small EVs and physically resemble small EVs. (a) Median size of transfection complexes and electroporated siRNA (a) before and (b) after differential centrifugation compared to NSC-34 (n=9) and HEK 293T (n=6) sEVs. Statistics: One-way ANOVA Dunnett's multiple comparisons test in relation to sEVs. (c-g) Particle size distribution of differentially centrifuged (c) siRNA (n=1), (d) electroporated siRNA (n=2) and transfection complexes made with (e) RNAiMAX (n=2), (f) INTERFERin (n=2) and (g) RiboJuice (n=1) relative to total amount of particles compared to HEK 293T sEVs (n=6). Statistics: Two-way ANOVA Dunnett's multiple comparisons test in relation to HEK 293T sEVs. (h) Absolute GFP siRNA copies recovered from differentially centrifuged siRNA, electroporated siRNA and transfection complexes relative to copies recovered from Trizol RNA isolation of spike-in of the initial amount of copies which was added to each sample. (n=3) Statistics: One-way ANOVA Dunnett's multiple comparisons in relation to Opti-MEM.

but not median sizes alone, were able to discriminate differences between some, but not all transfection complexes and sEVs.

The GFP siRNA, detected by RT-qPCR after differential centrifugation of transfection complexes made with RNAiMAX and INTERFERin, was significantly higher than background levels determined by processing of transfection complex media alone by the same sEV isolation protocol. This supports the hypothesis that intact transfection complexes made with RNAiMAX and INTERFERin are pelleted by the sEV isolation protocol. The percentage of siRNA copies from the initial amount of siRNA added to transfection complexes was determined to demonstrate the recovery. This was done by spiking Trizol with the amount of GFP siRNA copies used to make the transfection complexes to account for the poor recovery caused by Trizol extraction particularly with samples containing small amounts of RNA (demonstrated later in **Figure 11f**). The number of copies recovered from this control was compared to the number of copies recovered from the differentially centrifuged transfection complexes (**Figure 10h**). The recovery of siRNA ranged between 1-6% of the initial amount. It is possible that recovery is low as transfection complexes may be poorly recovered by differential centrifugation, as only about 25% of similarly sized sEVs are recovered with this protocol.

In short, differentially centrifuged transfection complexes made with RNAiMAX and INTERFERin resulted in detection of particles by NTA and siRNA by RT-qPCR that resemble sEVs. This implies that, if transfection complexes are released with sEVs, they would pellet with them and be detected like them. The transfection complexes have a similar median size to sEVs and thus cannot be separated by this characteristic. However, size distribution was able to distinguish differences between INTERFERin transfection complexes and sEVs. On the other

hand, size distribution was not able to reveal differences between RNAiMAX transfection complexes and sEVs.

Transfection complexes protect siRNA from RNase similarly to sEVs

RNase treatments were previously used to demonstrate that siRNAs are protected as they are located within sEVs. The siRNA protected by transfection complexes could account for the protection of siRNA observed in sEVs preparations. Transfection complexes were treated with RNase to determine their ability to protect siRNA. RNase treatment of GFP siRNA alone degraded all RNA with or without the presence of detergent (**Figure 11a**). Similarly, only 2% and 1% of GFP siRNA copies remained when electroporated GFP siRNA was treated with RNase or RNase + detergent (**Figure 11b**). This implies that the electroporation conditions used here do not cause the siRNA to aggregate and resist degradation. On the other hand, siRNA remained partly protected when the RNase treatment is applied to GFP siRNA complexed with RNAiMAX and INTERFERin while pretreatment with detergent resulted in nearly complete degradation (**Figure 11c,d**). RiboJuice's protective effect was less evident in the presence of RNase (**Figure 11e**). This would suggest that Ribojuice doesn't efficiently protect the siRNA and this could contribute to lower transfection efficiency. The recovery of RNA from untreated transfection complexes was compared to the initial amount of siRNA added to the transfection reagents. This illustrated that Trizol isolation poorly recovers the GFP siRNA (never higher than 3%) (**Figure 11f**). This would imply that siRNA copies are greatly underestimated in all RNA extractions, affecting sEV copy numbers. In summary, RNAiMAX and INTERFERin transfection complexes seem to protect siRNA from RNase similarly to sEVs. It is possible that these transfection complexes can be found in sEV preparations from transfected cells and partly explain the sensitivity of siRNA to RNase degradation in sEVs prepared from transfected cells.

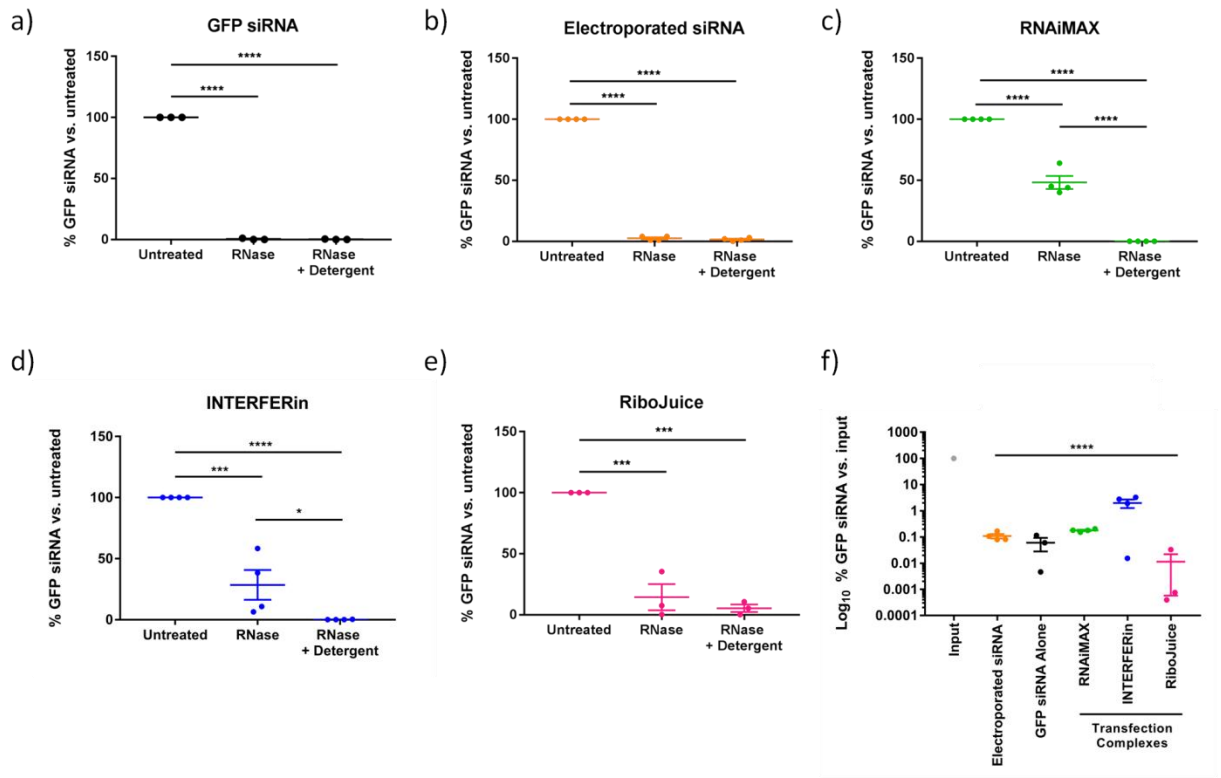

FIGURE 11. Transfection complexes can protect siRNA against RNase like small EVs. (a-d) Absolute GFP siRNA copies in RNase +/- detergent-treated (a) siRNA (n=3), (b) electroporated siRNA (n=4), and transfection complexes made with (c) RNAiMAX (n=4), (d) INTERFERin (n=4) and (e) RiboJuice (n=3) relative to untreated counterparts. Statistics: One-way ANOVA Tukey's multiple comparisons test. (f) Absolute GFP siRNA copies recovered from untreated samples relative to initial amount of copies added to each sample. Statistics: One-way ANOVA Dunnett's multiple comparisons test in relation to input.

Therefore, the protection of some siRNA by RNase in sEV preparations from transfected cells cannot be attributed entirely with certainty to sEVs.

Although the above evidence suggests that RNAiMAX and INTERFERin transfection complexes would pellet and mimic sEVs if they were exocytosed from transfected cells, what proportion of sEV-sized particles they account for in sEV preparations made using differential centrifugation is to be determined.

Small EVs released by transfected and untransfected cells differ

As demonstrated above, the size distribution profile of differentially centrifuged RNAiMAX transfection complexes was not significantly different from HEK 293T sEVs. The un-centrifuged transfection complexes were compared to their centrifuged counterpart (**Figure 12a**). There are significantly more 45 nm sized-particles and less 135 and 165 nm particles in the un-centrifuged transfection complexes compared to their centrifuged counterpart. This indicated the 45 nm transfection complexes were not pelleted during centrifugation or fusion to create larger particles occurred thus, resulting in similar distribution profiles to sEVs. sEVs produced by untransfected and transfected HEK 293T cells (RNAiMAX/GFP siRNA) were compared to determine if the size distribution of sEVs changes in transfected cells. The sEVs originating from transfected HEK 293T had a significant decrease in particles of 105 nm bins and an increase in particles in 225 and 255 nm (**Figure 12b**). This supports the idea that transfected cells produce larger particles. As mentioned earlier, differentially centrifuged RNAiMAX transfection complexes had a similar size distribution to untransfected sEVs whereas here we showed that transfected cells release larger sEVs. We hypothesize that the transfection complexes may fuse with sEVs, creating a larger hybrid vesicle.

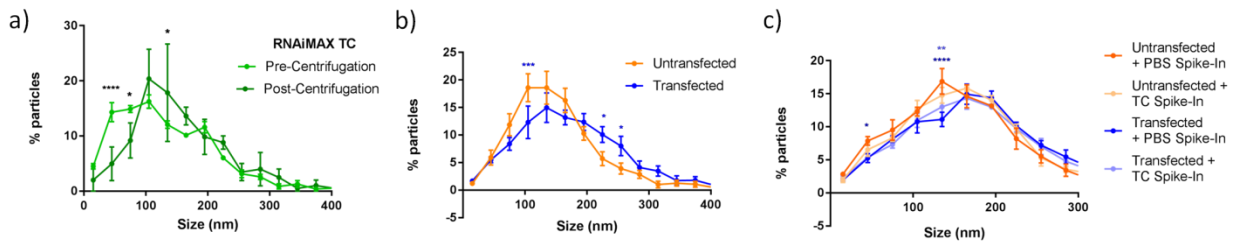

FIGURE 12. Particle size distribution of transfection complexes and small EVs originating from untransfected and transfected HEK 293T. (a) Size distribution of particles from transfection complexes (TC) pre- (n=4) and post-centrifugation (n=2) relative to total amount of particles. Statistics: Two-way ANOVA Sidak's multiple comparisons (b) Size distribution of particles from transfected (n=6) and untransfected (n=3) cells relative to total amount of particles. Statistics: Two-way ANOVA Sidak's multiple comparisons test in relation to small EVs originating from untransfected cells. (c) Size distribution of small EVs from untransfected and transfected cells +/- RNAiMAX TC spiked in prior to differential centrifugation. (n=4) Statistics: Two-way ANOVA Dunnett's multiple comparisons test in relation to small EVs originating from untransfected cells with PBS spiked in prior to differential centrifugation.

Small EVs from untransfected HEK 293T or HEK 293T transfected with RNAiMAX were isolated. PBS or transfection complexes were spiked-in to the collected media prior to differential centrifugation in order to determine if the sEVs potentially fuse with the transfection complexes. The size distribution profile revealed that whether transfection complexes are spiked-in or used to transfect cells, a shift occurs towards larger particles in sEV preparations (**Figure 12c**). This may indicate that transfection complexes fuse with sEVs to produce larger particles. Therefore, transfected cells may release these hybrid sEV-transfection complex vesicles or the hybrids may form after release of both transfection complexes and sEVs.

Transfection of cells affects the delivery of siRNA by sEVs

If transfection complexes contaminate or fuse with the sEVs, the ability of sEVs to deliver siRNA may be affected. To verify this, sEVs produced by wild-type (WT) HEK 293T, sEVs produced from a stable HEK 293T cell line which expresses GFP siRNA in the pre-miR-451 backbone as well as sEVs produced by the same stable cell line transfected with an irrelevant control siRNA were isolated. These sEVs were compared for their ability to knockdown GFP by incubating them with GFP NHDF-Neo cells and measuring fluorescence. Small EVs produced by the GFP siRNA-expressing cells should be able to knockdown GFP according to Reshke et al. (2019). On the other hand, the sEVs collected from these cells transfected with a scramble siRNA will be able to identify if transfection of sEV-producing cells alters the siRNA packaging and ability of sEVs to delivery GFP siRNA and knockdown GFP. When HEK 293T expressing GFP siRNA were transfected with a scramble siRNA and RNAiMAX, the ability of the resulting sEV preparations to knockdown GFP in GFP NHDF-Neo was reduced compared to sEVs originating from untransfected cells (**Figure 13a**). No significant differences were observed in concentrations or median sizes of the sEV preparations between transfected and untransfected cells (**Figure 13b,c**).

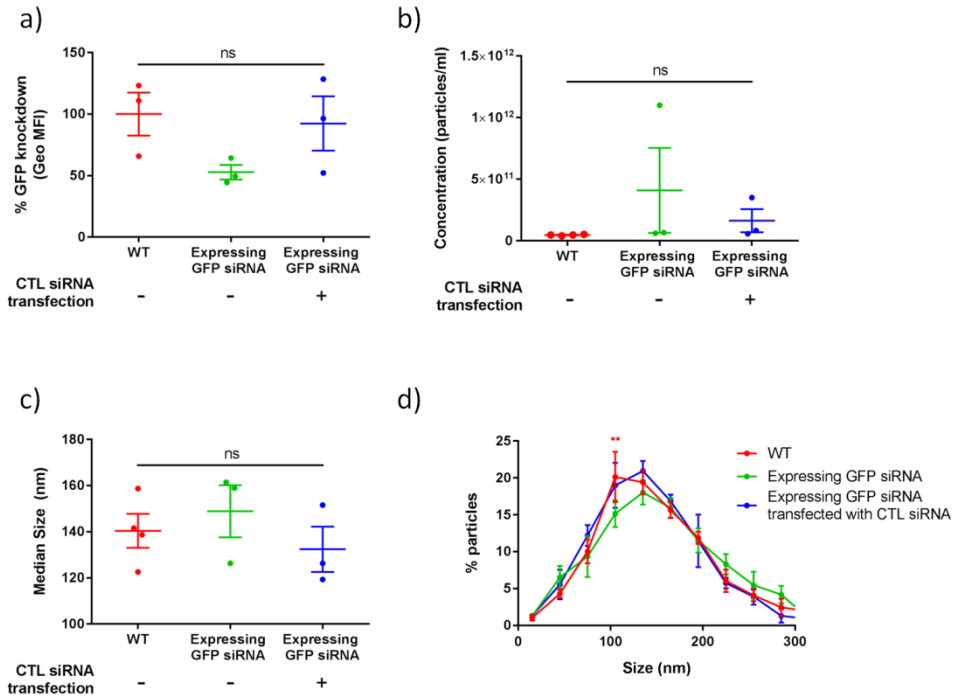

FIGURE 13. Comparing delivery capabilities of sEVs originating from transfected and untransfected cells. (a) Relative GFP knockdown of NHDF-Neo GFP cells treated with sEVs produced by untransfected and transfected HEK 293T expressing GFP siRNA in a pre-miR-451 backbone. Geometric mean fluorescence intensity was normalized to NHDF-Neo GFP cells treated with small EVs produced by WT HEK 293T. (n=3) Statistics: One-way ANOVA Dunnett's multiple comparisons test in relation to treatment with WT HEK 293T sEVs (b) Particle concentration. (n=3) Statistics: One-way ANOVA Tukey's multiple comparisons test. (c) Median size of particles. (n=3) Statistics: One-way ANOVA Tukey's multiple comparisons test. (d) Size distribution of particles in relation to total number of particles. (n=3) Statistics: Two-way ANOVA Dunnett's multiple comparisons test in relation to HEK 293T expressing GFP siRNA.

Discussion

This thesis attempted to transfect small extracellular vesicle-producing cells to package RNAs inside small EVs (sEVs). This method is often used and seemed to be the best option for loading chemically modified RNAs in sEVs. Chemical modifications are able to extend silencing of targets due to their increased stability and specificity[6–8]. Therefore, using a method to package chemically modified RNAs in sEVs is important for attempting to prolong the effect of RNAi therapeutics in tissues other than liver.

Initially, we demonstrated that chemical modifications present challenges to the use of standard methods to quantify RNA such and RT-qPCR. The miScript II RT-qPCR did not accurately measure the equal amounts, according to A_{260}, of SOD1-targeting RNAs and had a large bias towards unmodified ssRNA potentially due to its lack of secondary structures and chemical enhancements. TaqMan Small RNA Assay, however, was minimally affected by chemical modifications in the ssRNA. This suggests spectrophotometers can accurately measure concentrations of modified RNA and that annealing of primers and probes is not hindered by the chemical modifications, in agreement with the ability of these modified RNAs to bind complementary targets when used as therapeutics. TaqMan Small RNA Assay uses a hairpin primer complementary to our SOD1-targeting RNAs to initiate cDNA synthesis whereas miScript II RT kit polyadenylates the RNA prior to initiation of cDNA synthesis with an oligo-dT primer. Therefore, the lack of amplification of modified ssRNA and hairpin RNAs with miScript II RT-qPCR could be attributed to the structure and 3' modifications preventing poly(A) polymerase from accessing and polyadenylating the 3' end. This lack of polyadenylation would prevent initiation of cDNA synthesis by oligo-dT primer annealing. We concluded that TaqMan Small RNA Assay was the better method of the two for quantifying the SOD1-targeting RNAs. However, it was equally inefficient at amplifying the hairpin RNAs. This could be

explained by overestimation of its concentration by absorbance due to hyperchromicity or the hairpin primer's access to its target being obstructed. Hyperchromicity is the phenomenon that causes the absorbance of 2 single strands to be higher than when they are annealed thus should be considered for quantification of the hairpin and SOD1 siRNA as they mostly contain stacked bases. Spectrophotometers, like the Nanodrop use the Beer-Lambert law ($A=\text{Ɛ}Cl$) to determine nucleic acid concentrations. The 40 ng-cm/μ extinction coefficient (Ɛ) is used for RNA. Absorbance values can be corrected to account for the altered absorbance due to structures by using extinction coefficients custom to each RNA instead of using the default extinction coefficient. Calculated extinction coefficients varied concentrations by 10-25% (not shown). Therefore, extinction coefficients custom to each RNA should be used to measure their concentrations by absorbance and thus enabling transfection of each RNAs at equal amounts. However, the absorbance alone would not account for the 300-6,000 fold difference between the ssRNA and hairpin RNA. This finding suggests the hairpin structure is predominantly responsible for the impairment of RT-qPCR. Temperatures were not sufficiently high to unfold the hairpin RNA resulting in the inability of the RT primer to efficiently access and anneal to its target site concealed in the hairpin of the 42 nt pre-miRNA structure. The effect of structures of RNAs on RT-qPCR such as the hairpins found in pre-miRNA or tRNA structures may not be appreciated in the literature leading to assumptions that these RNAs are not abundant or present when interpretation revolves around RT-qPCR analysis.

We later saw by northern blot that both the unmodified and modified hairpin RNAs were being processed into shorter, likely single-stranded forms once transfected in cells. TaqMan Small RNA Assay isn't able to distinguish between these forms. However, we know that the linear SOD1 siRNA is the form better detected by RT-qPCR. Perhaps quantification via northern

blot or an RT-qPCR targeting specifically the 3’ end of the hairpin would help identify the fraction of hairpin and short linear forms in cells. The latter method could be applied to RNA isolated from sEVs to help determine which forms are most abundant in sEV preparations as insufficient RNA was isolated from sEV preparations to be visualized by northern blot. Similarly, a qPCR to detect the passenger strand of the siRNA could reveal if the siRNA is released with its passenger strand. Understanding whether an RNA in sEVs is a hairpin, dsRNA or linear will have a very large impact on interpretation of any quantitative data in sEVs.

TaqMan Small RNA Assay was used to quantify the SOD1-targeting RNAs in transfected cells and their sEVs. This revealed that unmodified ssRNA and siRNA had high levels in sEV preparations and that these levels were also higher in the transfected cells compared to the other small RNAs. This indicated that the modifications could be affecting the formation of transfection complexes, uptake of transfection complexes by cells, or escape of RNA into the cytoplasm. Even though the levels of SOD1-targeting RNA in cells transfected with unmodified hairpin seem to follow this trend of having higher levels in cells than its modified transfected counterpart, this cannot be confirmed since the hairpin RNA is processed in the Dicer-independent manner. The rate of conversion of the hairpin into single stranded 22 nt RNAs may vary between the modified and unmodified hairpins, complicating the accurate quantification and comparison of these RNAs in cells since TaqMan Small RNA Assay amplifies the hairpin and short linear forms at different efficiencies. In conclusion, uptake of chemically modified RNAs seemed hindered for transfection of modified ssRNA and siRNA.

Besides differences in efficiency at forming transfection complexes and being internalized, other variables, such as the stability of RNAs may help to explain the increase of certain RNAs in sEV preparations or cells over others. We could assume that the siRNA or

hairpins are more stable than the ssRNA. This would explain why the cells transfected with siRNA have higher levels of the SOD1-targeting RNA, as did their sEVs. Other factors include the varying abilities in escaping the endosome or the level of engagement in RNA silencing. Studies have demonstrated that single stranded RNA (ssRNA) are able to silence gene expression but are less potent than double stranded RNA (dsRNA) like siRNA[60]. Additionally, Lima et al. demonstrated that ssRNA and dsRNA have different affinities for Dicer and Argonaute which suggests that methods to minimize the engagement of RNAs in RNA silencing could enhance their packaging into sEVs[61,62]. In other words, this may indicate that changes in RNA structures lead to different rates of RNAi or exocytosis through sEVs. Therefore, a high knockdown may indicate silencing RNAs are retained in cells in active Argonaute complexes and their loading and release with sEVs is therefore reduced. In the case of the SOD1-targeting RNAs, these experiments used the mouse NSC-34 cells which do not contain the human SOD1; the target of the RNAs. Therefore, the levels of specific RNAs in sEV preparations may be entirely due to higher levels of transfection complex formation/uptake and not related to their engagement in the RNAi pathway. However, this can be tested. In order to test the impact of a target mRNA on packaging of siRNA into sEVs, these experiments could be repeated in human cells such as HEK 293T cells with or without genetic deletion of SOD1. Therefore, after introduction of the RNAs, mRNA levels would be measured to quantify knockdown as SOD1 has a long half-life (~20 days). The level of knockdown and copy numbers in sEV preparations could be calculated relative to one another to demonstrate if abundance in the cytoplasm solely dictates the rate of siRNA present in sEV preparations and if engagement in RNAi mechanisms affects RNA export in sEVs. Similarly, perhaps different amounts of co-localization with endosome markers would vary between single stranded, double stranded and hairpin RNAs. In

conclusion, many factors may be affecting the abundance of certain RNAs in sEV preparation; formation of transfection complexes or uptake by cells, resistance to nucleases, endosome escape and their engagement in the RNAi mechanism.

In the second half of the thesis, different transfection methods for packaging of RNAs into sEVs were compared since transfection efficiency correlated with the amount of SOD1-targeting RNAs in sEV preparations. Increasing transfection efficiency of chemically modified RNAs could, therefore, maximize the availability of RNAs in the cytoplasm for packaging into sEVs. For this reason, efficiency was determined by silencing of the mRNA target which occurs in the cytoplasm. We saw that naked siRNA was unable to silence the GFP mRNA without reagents. Additionally, a 10 nM siRNA concentration produced the best knockdown with all transfection methods however a plateau of GFP knockdown was beginning to form between the 5-10 nM siRNA concentrations. We speculate that this was due to siRNA saturation instead of saturation of the transfection reagents. This is supported by the fact that the first transfections with SOD1-targeting siRNA used 10 times less transfection reagent than the GFP siRNA transfections, yet still resulted in much higher levels of SOD1 siRNA copies in sEV preparations compared to the GFP siRNA (25 copies per sEV versus 1 copy per 7 sEVs). However, the lower GFP siRNA copy number could result from many things such as 1) different siRNAs transfecting/loading into sEVs differently, 2) the larger time span of collecting media post-transfection could mean GFP siRNA-containing sEVs are diluted with WT sEVs if the GFP siRNA packaging and release in sEVs occurs at a particularly short time period or 3) prior experiments were achieved by collecting media from two 10 cm plates per siRNA construct whereas the new experiments collected media from two 15 cm plates which encompass more media. sEV-sized contaminants in the media would thus increase and in turn increase the particle

concentration by nanoparticle tracking which would decrease the copy number (**supplementary 3**). RNAiMAX produced the highest knockdown and resulted in the production of the highest siRNA copy number in the sEV preparation. These results support that transfection efficiency is correlated with abundance of transfected RNAs in sEV preparations.

All three transfection reagents are cationic suggesting they interact with nucleic acids and the cellular membrane in related ways. However, as their components are different, details of their complex formation, their uptake and endosome escape may vary. Differences in transfection complex formation may correlate with their ability to protect the siRNA from RNase. RNAiMAX and INTERFERin transfection complexes seemed to protect siRNA better than RiboJuice which also had much lower silencing effects then the former. Also, different transfection complexes may be internalized by different endocytic pathways; for example, clathrin- or caveolin-dependent and clathrin-independent endocytosis or macropinocytosis. In each of these pathways, the transfection complexes may arrive in endosomes. The endosome can make its way back to the plasma membrane or deliver to the Golgi network to release the transfection complexes in the extracellular space[63]. RNA in transfection complexes may escape the endosome and get packaged in sEVs such as exosomes and microvesicles by the inward budding of the MVB or the outward budding of the cell membrane respectively. The early endosome, containing endocytosed transfection complexes, can also mature into multivesicular bodies which can also release their cargo once they fuse with the cell membrane. Late endosomes may also fuse with lysosomes and under stressed conditions the lysosomes may undergo exocytosis leading to the release of their undigested cargo[63]. Therefore, the transfected siRNA are likely not only getting exocytosed through the pathway of packaging into exosomes or microvesicles. More importantly, this suggests that transfection complexes themselves can be

exocytosed. Sahay et al. reported that ~70% of internalized lipid-siRNA complexes were exocytosed through the MVB recycling pathway[64]. This is supported by our finding that some of the endocytosed siRNA co-localizes with a late endosome, lysosome and exosome maker. The possibility of transfection complexes contaminating sEV preparations is very worrisome as it could lead to making false assumption about sEVs, putting into question the previous studies which used this method for sEV packaging.

RNase treatments were used to demonstrate that siRNA is protected because they are located inside sEVs. RNAiMAX transfection led to the release of more protected siRNA compared to the other methods. When cells were transfected with RNAiMAX, we saw 66% of the unmodified SOD1 siRNA and ~45% of the GFP siRNA was protected in sEV preparations. As listed above, transfected siRNA may be exocytosed through different pathways and this fate may vary according to the transfection method used. Therefore, siRNA may be released from cells attached to the surface of sEVs, released independent of vesicles, or released due to cell death or compromised sEV membranes due to the experimental protocol. Release of siRNA in sEVs, protein complexes or transfection complexes would protect the siRNA, as we observed, and lead to overestimated copy numbers. Therefore, the RNase protection assay commonly used to demonstrate that RNAs are protected inside sEVs cannot differentiate whether this RNA is protected due to sEVs, transfection complexes or other protein complexes.

If transfection complexes are being released alongside sEVs, we demonstrated that they would co-precipitate with sEVs as their median sizes are similar. However, analysis of the size distribution of sEVs and centrifuged INTERFERin-siRNA complexes or electroporated siRNA differed. Centrifuged RNAiMAX transfection complexes, on the other hand, were very similar to

the sEVs' distribution profile. Therefore, if these RNAiMAX transfection complexes were released alongside sEVs they would not be distinguishable from the sEVs.

We tracked fluorescently-labeled siRNA complexed with RNAiMAX into late endosomes and lysosomes. It is difficult to differentiate in this system whether siRNA is blocked in these endolysosomal compartments with transfection complexes or escaped into the cytoplasm and was packaged into exosomes at late endosomes. Labeling transfection reagents, as well as the siRNA they complex with, may allow one to track components of the transfection reagents to determine if these also localize in late endosomes. This may support the idea that transfection complexes as a whole get exocytosed.

Although RNAiMAX transfection complexes were similar to sEVs by NTA, when comparing sEVs released by untransfected versus RNAiMAX-transfected cells, we saw changes in the distribution profiles and abilities to deliver siRNA. Whether cells were transfected with RNAiMAX transfection complexes or the complexes were spiked-in prior to ultracentrifugation, there was an increase in particle sizes collected. This seemed to suggest that transfection complexes may fuse with the sEVs creating a larger hybrid. Transfection complexes could fuse with sEVs in late endosomes or after release from cells to produce the larger sEVs we saw in sEV preparations collected from transfected cells compared to untransfected cells. It has been reported that a simple incubation of lipofectamine transfection reagents with small EVs resulted in larger hybrid vesicles[50], as we observed. Alternatively, the components of the transfection complexes may dissociate in transfected cells and integrate in cellular or sEV membranes. In the event that transfection complexes dissociate, it is also possible that some of the transfection components are incorporated during sEV synthesis or packaged within the sEVs thus altering the content or nature of sEV membranes. Whether sEVs fuse with transfection complexes or the

components of transfection complexes are incorporated to sEVs, transfection itself affects the ability to package and deliver their content.

At the time of submission of this thesis, transfection complexes and sEVs collected from transfected and untransfected cells were sent for mass spectrometry-based lipidomics studies. This has the purpose of identifying whether lipids unique to transfection complexes are present in sEV preparations and to estimate the proportion of transfection complexes or their components in these preparations. This would confirm whether lipids in transfection complexes are exocytosed and contaminate sEV preparations. Electron microscopy of these same samples may verify if intact transfection complexes can be distinguished from sEVs and whether they seem to fuse together.

In conclusion, we demonstrate that transfection efficiency was correlated with RNA levels in sEV preparations. We saw that transfected siRNA co-localized with the late endosomes where sEVs such as exosome are produced suggesting that they are released with sEVs; either inside of them or complexed with other non-sEV entities such as the transfection reagents they are initially complexed with. Differentially centrifuged transfection complexes made with RNAiMAX were shown to be undistinguishable by NTA from sEVs isolated from untransfected cells. However, sEVs secreted by RNAiMAX-transfected cells differed from sEVs originating from untransfected cells. The increase in size of the sEVs resulting from transfection possibly indicates the fusion of transfection complexes with sEVs which may also explain the altered delivery capabilities of the sEVs coming from transfected cells. Therefore, transfection complexes or fusions of transfection complexes with sEVs may be a major contaminant of sEV preparations from transfected cells. This is likely a major confounding factor in a significant amount of published literature since transfection of EV-producing cells is a widely used method

for packing RNAs in sEVs[41–45]. Controls to account for transfection complexes aren`t considered and the experiments were not replicated with other methods of introducing RNA into sEVs to confirm the findings. For example, Liang et al. determined through microarray profiling that miR-125a was enriched in mesenchymal stem cell sEVs. They investigated whether the sEVs transfer this miRNA to recipient cells by transfecting the miR-125a or a miR-125a inhibitor RNA in mesenchymal stem cells using lipofectamine. The sEVs were collected using differential centrifugation and labeled with Dil to then be co-cultured with HUVEC cells. If transfection complexes contaminate sEV preparations, they would also be stained by the dye. Therefore, transfection complexes may be in part responsible for the presence of the fluorescent label of the miR-125a and Dil appearing in recipient cells co-cultured with the sEVs and the up-regulation of angiogenic genes and down regulation of anti-angiogenic genes. Similarly, transfection complexes could be taking part in the delivery of miR-125a inhibitor RNA causing the inverse effects seen. Therefore, transfection complexes may lead to misinterpretations of the ability of sEVs to deliver miRNA and modulate recipient cells. These findings then led other related studies to use similar methods to further evaluate miR-125a in sEVs[41]. Similarly, *Li* et al. transfected a scramble siRNA and an siRNA of interest in mesenchymal stem cells with lipofectamine. sEVs were collected and analyzed by western blot for markers, nanoparticle tracking (NTA) for size and electron microscopy (EM) for morphology. Detecting sEV markers does not verify the presence of potential contaminants such as transfection complexes. Additionally, NTA was only used to compare sEVs originating from cells transfected with scramble siRNA or transfected with the siRNA of interest. Therefore, untransfected cells were not verified to determine the possibility of contaminating transfection complexes. Lastly, the morphology of transfection complexes may not be different from sEVs. Therefore, the

conclusion that the siRNA delivered through sEVs sensitizes resistant cancer cells to Sorafenib may be a combined effort of sEVs and transfection complexes. All to say that transfection of sEV-producing cells may not be a reliable method to package RNA in sEVs as it changes the sEVs produced leading to misrepresentation of sEV population. Other methods which do not use transfection complexes, such as electroporation, or stable expression of RNAs in cells may avoid these issues.

References

1. Czech, B. & Hannon, G. J. Small RNA sorting: matchmaking for Argonautes. *Nat. Rev. Genet.* **12**, 19–31 (2011).
2. Bartlett, D. W. & Davis, M. E. Insights into the kinetics of siRNA-mediated gene silencing from live-cell and live-animal bioluminescent imaging. *Nucleic Acids Res.* **34**, 322–33 (2006).
3. Gantier, M. P. *et al.* Analysis of microRNA turnover in mammalian cells following Dicer1 ablation. *Nucleic Acids Res.* **39**, 5692–5703 (2011).
4. Van Rooij, E. *et al.* Control of stress-dependent cardiac growth and gene expression by a microRNA. *Science (80-.).* **316**, 575–579 (2007).
5. Lam, J. K. W., Chow, M. Y. T., Zhang, Y. & Leung, S. W. S. siRNA versus miRNA as therapeutics for gene silencing. *Molecular Therapy - Nucleic Acids* **4**, e252 (2015).
6. Nair, J. K. *et al.* Impact of enhanced metabolic stability on pharmacokinetics and pharmacodynamics of GalNAc-siRNA conjugates. *Nucleic Acids Res.* **45**, 10969–10977 (2017).
7. Engels, J. W. Gene silencing by chemically modified siRNAs. *N. Biotechnol.* **30**, 302–307 (2013).
8. Judge, A. D. *et al.* Sequence-dependent stimulation of the mammalian innate immune response by synthetic siRNA. *Nat. Biotechnol.* **23**, 457–462 (2005).
9. Fitzgerald, K. *et al.* A Highly Durable RNAi Therapeutic Inhibitor of PCSK9. *N. Engl. J. Med.* **376**, 41–51 (2017).
10. Roundtree, I. A., Evans, M. E., Pan, T. & He, C. Dynamic RNA Modifications in Gene Expression Regulation. *Cell* **169**, 1187–1200 (2017).
11. Watts, J. K., Deleavey, G. F. & Damha, M. J. Chemically modified siRNA: tools and

applications. *Drug Discov. Today* **13**, 842–855 (2008).

12. Morrissey, D. V. *et al.* Potent and persistent in vivo anti-HBV activity of chemically modified siRNAs. *Nat. Biotechnol.* **23**, 1002–1007 (2005).
13. Watts, J. & Corey, D. Gene silencing by siRNAs and antisense oligonucleotides in the laboratory and the clinic. *J. Pathol.* **226**, 365–379 (2012).
14. Dar, S. A., Thakur, A., Qureshi, A. & Kumar, M. SiRNAmod: A database of experimentally validated chemically modified siRNAs. *Sci. Rep.* **6**, 1–8 (2016).
15. Pei, Y. *et al.* Quantitative evaluation of siRNA delivery in vivo. *RNA* **16**, 2553–2563 (2010).
16. Veldhoen, S., Laufer, S. D., Trampe, A. & Restle, T. Cellular delivery of small interfering RNA by a non-covalently attached cell-penetrating peptide: Quantitative analysis of uptake and biological effect. *Nucleic Acids Res.* **34**, 6561–6573 (2006).
17. Wittrup, A. *et al.* Visualizing lipid-formulated siRNA release from endosomes and target gene knockdown. *Nat. Biotechnol.* **33**, 870–6 (2015).
18. Ganesan, P. & Narayanasamy, D. Lipid nanoparticles: Different preparation techniques, characterization, hurdles, and strategies for the production of solid lipid nanoparticles and nanostructured lipid carriers for oral drug delivery. *Sustainable Chemistry and Pharmacy* **6**, 37–56 (2017).
19. Gilleron, J. *et al.* Identification of siRNA delivery enhancers by a chemical library screen. *Nucleic Acids Res.* **43**, 7984–8001 (2015).
20. Reshke, R. *et al.* An RNA Stem-Loop Robustly Packages Silencing RNAs into Exosome-like Vesicles for Highly Efficient in vivo Delivery. *Revis. Submitt. to Nat. Biomed. Eng. June 2019*

21. Ozcan, G., Ozpolat, B., Coleman, R. L., Sood, A. K. & Lopez-Berestein, G. Preclinical and clinical development of siRNA-based therapeutics HHS Public Access. *Adv Drug Deliv Rev* **87**, 108–119 (2015).

22. Garber, K. Alnylam terminates revusiran program, stock plunges. *Nat. Biotechnol.* **34**, 1213–1214 (2016).

23. Kulkarni, J. A., Cullis, P. R. & Van Der Meel, R. Lipid Nanoparticles Enabling Gene Therapies: From Concepts to Clinical Utility. doi:10.1089/nat.2018.0721

24. Lorenzer, C., Dirin, M., Winkler, A. M., Baumann, V. & Winkler, J. Going beyond the liver: Progress and challenges of targeted delivery of siRNA therapeutics. *Journal of Controlled Release* **203**, 1–15 (2015).

25. Zhuang, X. *et al.* Treatment of Brain Inflammatory Diseases by Delivering Exosome Encapsulated Anti-inflammatory Drugs From the Nasal Region to the Brain. (2011). doi:10.1038/mt.2011.164

26. EL Andaloussi, S., Mäger, I., Breakefield, X. O. & Wood, M. J. A. Extracellular vesicles: biology and emerging therapeutic opportunities. *Nat. Rev. Drug Discov.* **12**, 347–357 (2013).

27. Raposo, G. & Stoorvogel, W. Extracellular vesicles: Exosomes, microvesicles, and friends. *J. Cell Biol.* **200**, 373–383 (2013).

28. Zhang, H. *et al.* Identification of distinct nanoparticles and subsets of extracellular vesicles by asymmetric flow field-flow fractionation. *Nat. Cell Biol.* **20**, 332–343 (2018).

29. Ma, L. *et al.* Discovery of the migrasome, an organelle mediating release of cytoplasmic contents during cell migration. *Cell Res.* **25**, 24–38 (2015).

30. Ashley, J. *et al.* Retrovirus-like Gag Protein Arc1 Binds RNA and Traffics across

Synaptic Boutons. *Cell* **172**, 262-274.e11 (2018).

31. Pastuzyn, E. D. *et al.* The Neuronal Gene Arc Encodes a Repurposed Retrotransposon Gag Protein that Mediates Intercellular RNA Transfer. *Cell* **172**, 275-288.e18 (2018).
32. Valadi, H. *et al.* Exosome-mediated transfer of mRNAs and microRNAs is a novel mechanism of genetic exchange between cells. *Nat. Cell Biol.* **9**, 654–659 (2007).
33. Jamaly, S. *et al.* Impact of preanalytical conditions on plasma concentration and size distribution of extracellular vesicles using Nanoparticle Tracking Analysis. *Sci. Rep.* **8**, (2018).
34. Théry, C. *et al.* Minimal information for studies of extracellular vesicles 2018 (MISEV2018): a position statement of the International Society for Extracellular Vesicles and update of the MISEV2014 guidelines. *J. Extracell. Vesicles* **7**, (2018).
35. Théry, C., Amigorena, S., Raposo, G. & Clayton, A. Isolation and Characterization of Exosomes from Cell Culture Supernatants and Biological Fluids. *Curr. Protoc. Cell Biol.* **30**, 3.22.1-3.22.29 (2006).
36. Patel, G. K. *et al.* Comparative analysis of exosome isolation methods using culture supernatant for optimum yield, purity and downstream applications. *Sci. Rep.* **9**, (2019).
37. Guduric-Fuchs, J. *et al.* Selective extracellular vesicle-mediated export of an overlapping set of microRNAs from multiple cell types. *BMC Genomics* **13**, 357 (2012).
38. Chevillet, J. R. *et al.* Quantitative and stoichiometric analysis of the microRNA content of exosomes. *Proc. Natl. Acad. Sci.* **111**, 14888–14893 (2014).
39. Alvarez-Erviti, L. *et al.* Delivery of siRNA to the mouse brain by systemic injection of targeted exosomes. *Nat. Biotechnol.* (2011). doi:10.1038/nbt.1807
40. Kamerkar, S. *et al.* Exosomes facilitate therapeutic targeting of oncogenic KRAS in

pancreatic cancer. *Nature* (2017). doi:10.1038/nature22341

41. Wang, D. *et al.* Exosomes from mesenchymal stem cells expressing miR-125b inhibit neointimal hyperplasia via myosin IE. *J. Cell. Mol. Med.* **23**, 1528–1540 (2019).

42. Liu, Y. *et al.* AMSC-derived exosomes alleviate lipopolysaccharide/D-galactosamine-induced acute liver failure by miR-17-mediated reduction of TXNIP/NLRP3 inflammasome activation in macrophages. *EBioMedicine* **36**, 140–150 (2018).

43. Nojima, H. *et al.* Hepatocyte exosomes mediate liver repair and regeneration via sphingosine-1-phosphate. *J. Hepatol.* **64**, 60–68 (2016).

44. Wei, G. *et al.* Dendritic cells derived exosomes migration to spleen and induction of inflammation are regulated by CCR7. *Sci. Rep.* **7**, 1–9 (2017).

45. Li, H., Yang, C., Shi, Y. & Zhao, L. Exosomes derived from siRNA against GRP78 modified bone-marrow-derived mesenchymal stem cells suppress Sorafenib resistance in hepatocellular carcinoma. *J. Nanobiotechnology* **16**, 1–13 (2018).

46. Villarroya-Beltri, C. *et al.* Sumoylated hnRNPA2B1 controls the sorting of miRNAs into exosomes through binding to specific motifs. *Nat. Commun.* **4**, 1–10 (2013).

47. Santangelo, L. *et al.* The RNA-Binding Protein SYNCRIP Is a Component of the Hepatocyte Exosomal Machinery Controlling MicroRNA Sorting. *Cell Rep.* **17**, 799–808 (2016).

48. Mukherjee, K. *et al.* Reversible HuRmicroRNA binding controls extracellular export of miR122 and augments stress response. *EMBO Rep.* **17**, 11841203 (2016).

49. Kooijmans, S. A. A. *et al.* Electroporation-induced siRNA precipitation obscures the efficiency of siRNA loading into extracellular vesicles. *J. Control. Release* **172**, 229–238 (2013).

50. Lin, Y. *et al.* Exosome–Liposome Hybrid Nanoparticles Deliver CRISPR/Cas9 System in MSCs. *Adv. Sci.* **5**, 1–9 (2018).

51. Yang, S. *et al.* Conserved vertebrate mir-451 provides a platform for Dicer-independent, Ago2-mediated microRNA biogenesis. *Proc. Natl. Acad. Sci. U. S. A.* **107**, 15163–15168 (2010).

52. Cheloufi, S., Santos, C. O. Dos, Chong, M. M. W. & Hannon, G. J. A Dicer-independent miRNA biogenesis pathway that requires Ago catalysis. **465**, 584–589 (2010).

53. Cifuentes, D. *et al.* NIH Public Access. *Processing* **328**, 1694–1698 (2011).

54. Invitrogen. Mechanism of cationic lipid-mediated transfection. Available at: https://www.thermofisher.com/ca/en/home/references/gibco-cell-culture-basics/transfection-basics/gene-delivery-technologies/cationic-lipid-mediated-delivery/how-cationic-lipid-mediated-transfection-works.html.

55. Taylor, J. P., Brown, R. H. & Cleveland, D. W. Decoding ALS: from genes to mechanism. *Nature* **539**, 197–206 (2016).

56. Miller, R. G., Mitchell, J. D. & Moore, D. H. Riluzole for amyotrophic lateral sclerosis (ALS)/motor neuron disease (MND). *Cochrane Database Syst. Rev.* CD001447 (2012). doi:10.1002/14651858.CD001447.pub3

57. Abe, K. *et al.* Safety and efficacy of edaravone in well defined patients with amyotrophic lateral sclerosis: a randomised, double-blind, placebo-controlled trial. *Lancet Neurol.* **16**, 505–512 (2017).

58. Wang, H. *et al.* Therapeutic gene silencing delivered by a chemically modified small interfering RNA against mutant SOD1 slows amyotrophic lateral sclerosis progression. *J. Biol. Chem.* **283**, 15845–15852 (2008).

59. Ralph, G. S. *et al.* Silencing mutant SOD1 using RNAi protects against neurodegeneration and extends survival in an ALS model. *Nat. Med.* **11**, 429–433 (2005).

60. Lima, W. F. *et al.* Single-Stranded siRNAs Activate RNAi in Animals. *Cell* **150**, 883–894 (2012).

61. Lima, W. F. *et al.* Human Dicer binds short single-strand and double-strand RNA with high affinity and interacts with different regions of the nucleic acids. *J. Biol. Chem.* **284**, 2535–2548 (2009).

62. Lima, W. F. *et al.* Binding and cleavage specificities of human Argonaute 2. *J. Biol. Chem.* **284**, 26017–26028 (2009).

63. Dahiya, U. R. & Ganguli, M. Exocytosis - a putative road-block in nanoparticle and nanocomplex mediated gene delivery. *J. Control. Release* **303**, 67–76 (2019).

64. Sahay, G. *et al.* Efficiency of siRNA delivery by lipid nanoparticles is limited by endocytic recycling. *Nat. Biotechnol.* **31**, 653–658 (2013).

Supplementary

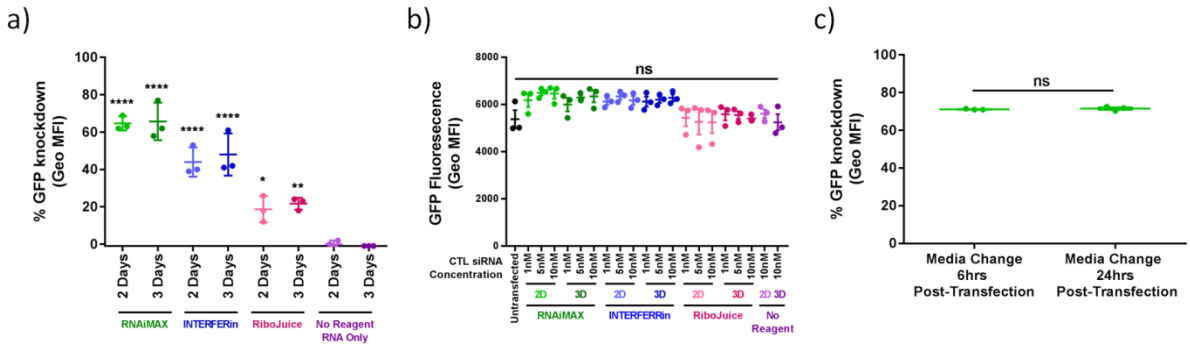

FIGURE 1. Controls for transfection with transfection reagents. (a) Relative GFP knockdown in HEK 293A GFP cells two and three days after transfection with 10 nM GFP siRNA +/- transfection reagents normalized to samples transfected with control siRNA and the associated reagent. (n=3) Statistics: Two-way ANOVA Dunnett's multiple comparisons test in relation to knockdown with no reagent. (b) Geometric mean fluorescence intensity two and three days after cells were transfected with various concentrations of scramble siRNA and transfection reagents. (n=3) Statistics: One-way ANOVA Tukey's multiple comparisons test. (c) Relative GFP knockdown in HEK 293A GFP cells three days after transfection with 10 nM GFP siRNA where media was replaced with fresh 6h or 24h after transfection. Geometric mean fluorescence intensity was normalized to samples transfected with control siRNA. (n=3) Statistics: Unpaired TTEST.

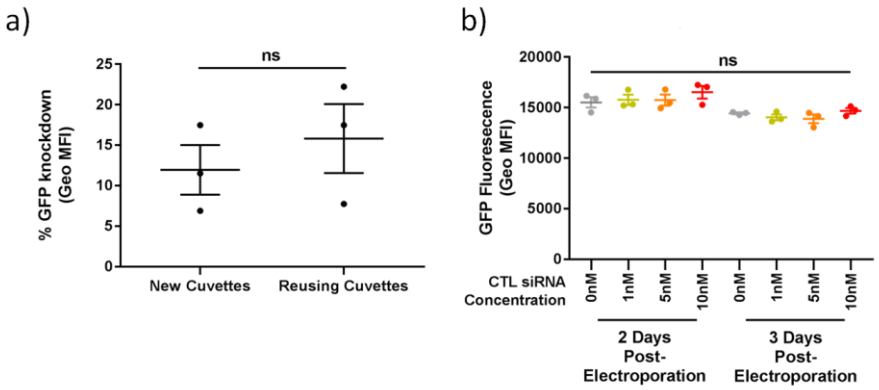

FIGURE 2. Controls for transfection via electroporation. (a) Relative GFP knockdown in HEK 293A GFP cells two days after electroporation of 5 nM GFP siRNA with new or reused cuvettes. Geometric mean fluorescence intensity was normalized to samples electroporated with control siRNA. (n=3) Statistics: Unpaired TTEST (b) Geometric mean fluorescence intensity of HEK 293A GFP cells transfected with various concentrations of scramble siRNA. (n=3) Statistics: Two-way ANOVA Tukey's multiple comparisons test.

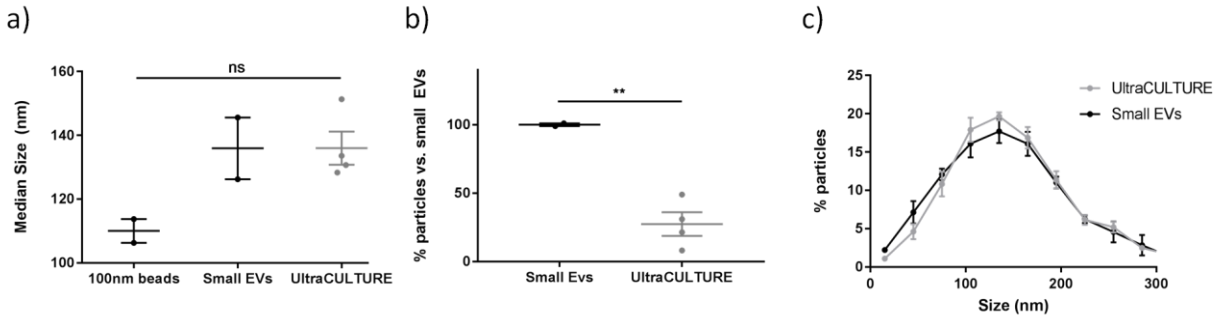

FIGURE 3. Small EV-like particles in ultraCULTURE. Differentially centrifuged ultraCULTURE from HEK 293T cells (n=2) or straight from stock bottle (n=4). (a) Median size of particles. Statistics: One-way ANOVA Tukey's multiple comparisons test (b) Particle concentration of ultraCULTURE relative to particle concentration of ultraCULTURE collected from HEK 293T cells. Statistics: Unpaired ttest. (c) Particle size distribution relative to total amount of particles. Statistics: Two-way ANOVA Sidak's multiple comparisons test.

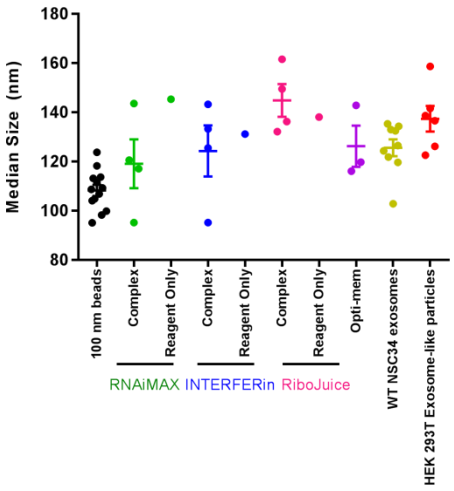

FIGURE 4. Median particle size of transfection reagents compared to transfection complexes.